Journal of Archaeological Science 190 (2026) 106561

Contents lists available at ScienceDirect

Journal of Archaeological Science

journal homepage: www.elsevier.com/locate/jas

Walking through the landscape: A different approach to mobility through $^{87}Sr/^{86}Sr$ isoscapes

Emma Stuart [a,*], Andrea Di Renzoni [b], Carmen Esposito [c], Luca Bondioli [d], Anna Cipriani [e,f], Alessia Nava [g], Federico Lugli [e], Alessandro Vanzetti [a,**]

[a] Department of Ancient World Studies, Sapienza University of Rome, Italy
[b] CNR-ISPC (National Research Council of Italy – Institute of Heritage Science), Italy
[c] Department of Cultural Heritage, University of Bologna, Ravenna, Italy
[d] Institute of Geological Sciences, Polish Academy of Sciences, Krakow Research Centre, Poland
[e] Department of Chemical and Geological Sciences, University of Modena & Reggio Emilia, Italy
[f] Lamont-Doherty Earth Observatory of Columbia University, Palisades, NY, United States of America
[g] Department of Odontostomatological and Maxillofacial Sciences, Sapienza University of Rome, Italy

ARTICLE INFO

Keywords:
$^{87}Sr/^{86}Sr$
Isoscape of Italy
Isochrones
Walking distance
Unusualness index

ABSTRACT

Strontium isotope analyses ($^{87}Sr/^{86}Sr$) represent a fundamental tool for reconstructing human mobility in the past. However, interpretations based on comparisons between the isotopic values of mineralised tissues and local baselines – reducing mobility to a simple "local" versus "non-local" dichotomy – may result in over-simplified views of complex phenomena. In fact, such an approach may blur the complexity of human movement and the non-linear relationships between individuals and the landscape in which they are ultimately buried. This study addresses these limitations by integrating $^{87}Sr/^{86}Sr$ isoscapes with two combined approaches: the use of isochrones, representing walking-time catchments around archaeological sites, and the Unusualness index, a statistical measure of deviation between human $^{87}Sr/^{86}Sr$ values and surrounding $^{87}Sr/^{86}Sr$ isoscape predictions. These methods are applied to two newly developed $^{87}Sr/^{86}Sr$ isoscapes of Italy, generated from an expanded dataset (n = 3096) of published environmental and archaeological samples, interpolated using Ordinary Kriging at 1 km grid size.

We evaluate the impact of including or excluding sample categories with potentially high isotopic variability in the construction of isotopic maps (e.g., humans, medium-large mammals), and highlight the importance of consistent preliminary data processing.

Two published Iron Age sites – Fermo (Esposito et al., 2023) and Monterenzio Vecchio (Sorrentino et al., 2018) – serve as case-studies to test this combined approach. By statistically evaluating the relationship between human samples and the isoscape values within the isochrones, we define three mobility classes, i.e., stable, circadian, and long-range ones, thereby contributing to the identification of more varied mobility patterns. This integrated framework demonstrates how the combination of isoscapes, isochrones, and the Unusualness index supports a nuanced, spatially sensitive understanding of past human mobility.

1. Introduction

The application of strontium ($^{87}Sr/^{86}Sr$) isotope analyses has become a pivotal tool in the archaeological field, allowing the reconstruction of complex aspects of past human behaviour, such as mobility and migration patterns (e.g., Knipper, 2009; Hedman et al., 2018; Madgwick et al., 2019; Schwartz et al., 2021). This methodology is founded on two key principles. Firstly, geological units are characterised by distinctive $^{87}Sr/^{86}Sr$ isotopic signatures, which derive from the radioactive decay of rubidium (Rb) within rocks and vary according to their age and

* Corresponding author.
** Corresponding author.
E-mail addresses: emma.stuart@uniroma1.it (E. Stuart), andrea.direnzoni@cnr.it (A. Di Renzoni), carmen.esposito2@unibo.it (C. Esposito), ndbondio@cyf-kr.edu.pl (L. Bondioli), anna.cipriani@unimore.it (A. Cipriani), alessia.nava@uniroma1.it (A. Nava), federico.lugli@unimore.it (F. Lugli), alessandro.vanzetti@uniroma1.it (A. Vanzetti).

https://doi.org/10.1016/j.jas.2026.106561
Received 17 May 2025; Received in revised form 9 February 2026; Accepted 31 March 2026
Available online 25 April 2026
0305-4403/© 2026 The Authors. Published by Elsevier Ltd. This is an open access article under the CC BY license (http://creativecommons.org/licenses/by/4.0/).

geological formation processes. These isotopes enter the environment through weathering processes, where they are absorbed by plants, animals, and humans (Toots and Voorhies, 1965; Parker, 1968; Parker and Toots, 1970; Schoeninger, 1979a, 1979b; Sillen, 1981; Ericson, 1985; de Laeter et al., 2003; Holt et al., 2021). While basically dependent on bedrock composition, bioavailable $^{87}Sr/^{86}Sr$ ratios (i.e., the ratios actually assimilated by living organisms) often deviate from those of the underlying bedrock due to the influence of other $^{87}Sr/^{86}Sr$ sources, such as atmospheric inputs and groundwater. This mixing results in a range of values known as the local baseline, which may not directly match bedrock signatures (Capo et al., 1998; Beard and Johnson, 2000; Frei and Frei, 2013; Adams et al., 2019; Hamilton et al., 2019; Britton et al., 2020; Gigante et al., 2023) (see Fig. 1). Secondly, any isotope fractionation of the $^{87}Sr/^{86}Sr$ ratio is corrected during mass spectrometry analysis, by normalising to a constant $^{88}Sr/^{86}Sr$ ratio. Consequently, the $^{87}Sr/^{86}Sr$ values measured in human or faunal tissues reflect the isotopic composition of the environment in which the tissues formed, provided that the intake of $^{87}Sr/^{86}Sr$ inputs was sufficiently stable – i.e., limited mobility or variability during tissue formation (Toots and Voorhies, 1965; Parker, 1968; Parker and Toots, 1970; Schoeninger, 1979a,b; Sillen, 1981; Ericson, 1985; Knudson et al., 2010; Lugli et al., 2022; but see Lazzerini et al., 2021 for the time required for a local end-member value to be incorporated in mineralised tissue).

If no contamination affects the tissues, comparing the human $^{87}Sr/^{86}Sr$ ratio of mineralised tissues formed at different stages of an individual's life with local baselines —constructed from environmental samples near archaeological sites— allows the identification of local and non-local individuals, or, in some cases, to track mobility shifts during an individual's life, depending on the analysed tissue. Such baselines are often derived from sampling with limited spatial coverage and tend to fail to account for the broader isotopic variability of surrounding and larger regions (Ericson, 1985; Slovak and Paytan, 2011; Lugli et al., 2022). To address these limitations, isotopic value distribution maps or "isoscapes" have been developed, with the aim of extending baseline data to regional scales, thus improving the ability to infer mobility patterns across diverse landscapes (Bowen, 2010; Holt et al., 2021; Lugli et al., 2022).

Isoscapes are built by interpolating into grids the uneven spatial distributions of bioavailable and geological $^{87}Sr/^{86}Sr$ values to predict isotopic ratios in uninvestigated areas (Bataille et al., 2020; Lugli et al., 2022). While the "smoothing effect" produced by interpolation may obscure sudden local variability, potentially leading to inaccuracies in mapping, isoscapes offer valuable insights into overall regional patterns. Acknowledging both their inherent limitations and strengths, recent decades have witnessed significant advancements in their development, employing geostatistical methods (e.g., Montgomery et al., 2006; Evans et al., 2010; Frei and Frei, 2011; Bataille and Bowen, 2012; Pestle et al., 2013; Hartman and Richards, 2014; Copeland et al., 2016; Kootker et al., 2016; Laffoon et al., 2017; Bataille et al., 2018; Hedman et al., 2018; Adams et al., 2019; Janzen et al., 2020; Ladegaard-Pedersen et al., 2022; Scaffidi and Knudson, 2020; Snoeck et al., 2020; Wang and Tang, 2020; Frank et al., 2021; Funck et al., 2021; Willmes et al., 2021; Lugli et al., 2022; Washburn et al., 2021; Gigante et al., 2023; Wang et al., 2023; Zaugg et al., 2023).

For Italy, Emery et al. (2018) produced a preliminary isoscape by interpolating literature data through inverse distance weighting (IDW). Subsequently, Lugli et al. (2022) employed Ordinary Kriging and Universal Kriging to interpolate a larger dataset comprising both original and published data, resulting in four maps: two based exclusively on bioavailable samples and two incorporating geological samples to the

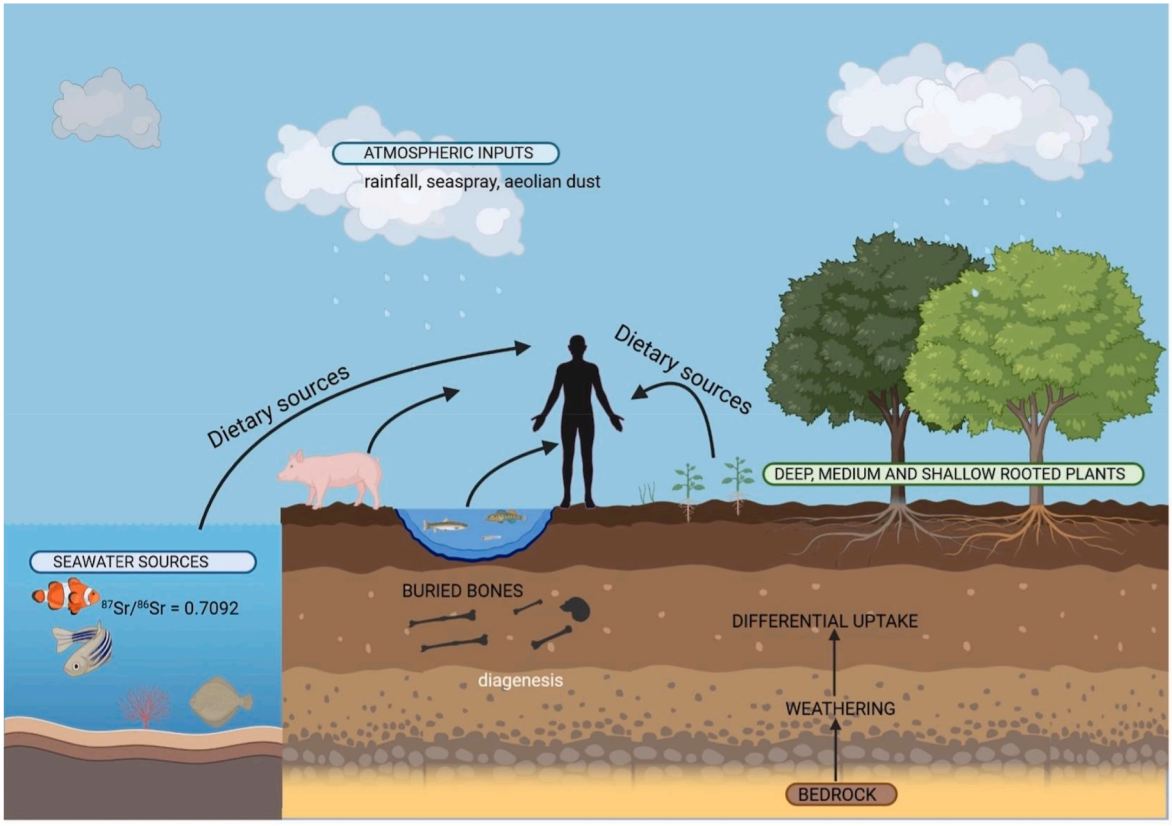

Fig. 1. The Strontium cycle from bedrock to the bioavailable portion of the environment.
Figure created with BioRender.com by Carmen Esposito. (For interpretation of the references to colour in this figure legend, the reader is referred to the Web version of this article.)

first. Gigante et al. (2023) developed an isoscape for southern Sardinia, employing a Random Forest machine-learning model based on bioavailable samples (plants). Another regional isoscape was developed by Zaugg et al. (2023), where plant and water samples from the Sybaris Region (Calabria) were processed through Ordinary Kriging. Defant et al. (2025) also recently contributed to the $^{87}Sr/^{86}Sr$ bioavailable coverage of Italy by creating an isoscape map with plant samples utilising AverageR, a Bayesian geo-statistical model.

Moreover, since the publication of the Italian isoscape by Lugli et al. (2022), several $^{87}Sr/^{86}Sr$ datasets have been published, concerning baselines for provenance analyses of specific case-studies (i.e., Sabatini et al., 2022; Esposito et al., 2023; Romboni et al., 2023) and $^{87}Sr/^{86}Sr$ mapping of specific areas (i.e., Ladegaard-Pedersen et al., 2022; Gigante et al., 2023; Zaugg et al., 2023). As isoscapes continue to gain prominence in archaeological research, critical questions regarding their construction and application have emerged. Recent studies and reviews (Bowen, 2010; Willmes, 2015; Bataille et al., 2020; Holt et al., 2021) have highlighted various challenges and uncertainties associated with using specific sample categories to build baselines and isoscapes, as well as broader concerns about their general applicability (e.g., Rossi et al., 2024).

Furthermore, it is necessary to consider the complexity of mobility and migration phenomena when reconstructing social and behavioural aspects of past populations using skeletal series (Gregoricka, 2021). Anthropological studies emphasise the continuum of temporary and long-term mobility, ranging from short-term seasonal movements and subsistence-driven migrations to more permanent, one-way relocations (Gregoricka, 2021). However, isotopic studies —constrained by the sampled tissue to a limited vision of movements in a lifetime— frequently reduce this complexity to a binary framework of "local" versus "non-local". This approach tends to give insights on large-scale migrations, while overlooking the smaller-scale, localised movements (Cabana and Clark, 2011; Cameron, 2013; Gregoricka, 2021). As a result, such studies often produce only a partial reconstruction of past human mobility and its interactions with the landscape. Yet mobility is inherently multifaceted, operating across diverse spatial and chronological scales. Human movement is shaped by dynamic interactions with the landscape and by the evolving social organisation of communities, necessitating analytical models and tools that accommodate this diversity and complexity.

This study has two primary aims: a) to critically evaluate the application of isoscapes by constructing two updated isotopic maps of the Italian peninsula and its major islands stemming from the isoscapes produced by Lugli et al. (2022). Through a step-by-step process of refining and updating the Italian isoscape, this research seeks to address and overcome some of the methodological challenges affecting the construction and use of such maps; b) to propose a more advanced approach to mobility research, aiming to overcome the binary categorisation of "local" versus "non-local" towards a more nuanced interpretation of the isotopic evidences. By considering the morphology of the territory interpreted as walking time (isochrones) with $^{87}Sr/^{86}Sr$ isoscapes and by using statistical methods applied to the latter and to isotopic ratio measurements on tissues (Unusualness index), this study examines mobility at multiple scales, interpreting it as a complex, non-linear phenomenon. While considering the strengths and limitations of isoscapes in provenance research, this paper aims to contribute to the conceptualisation of past mobility. Two Iron-Age case-studies —Fermo (Esposito et al., 2023) and Monterenzio Vecchio (Sorrentino et al., 2018)— have been selected to show the consistency of the proposed methods. In fact, although the aim of this study is not to compare the mobility patterns between these two archaeological sites, we think that discussing two practical cases, already presented in the literature, can be useful to demonstrate the applicability of the proposed method, and its differences with former analyses and interpretations.

2. Materials and methods

2.1. Materials: sample selection and database for the isoscapes

The dataset includes extensive data-gathering from literature (ending in 2023), encompassing both bioavailable and non-bioavailable samples (Table 1). Building upon the dataset provided by Lugli et al. (2022), an additional n = 1196 published samples were incorporated (Scheeres et al., 2013; Cangemi, 2016; Killgrove and Montgomery, 2016; Desideri, 2018; Emery et al., 2018; Grupe et al., 2018; Sorrentino et al., 2018; Cavazzuti et al., 2019a, 2019b; Arienzo et al., 2020; Francisci et al., 2020; Reinberger et al., 2021; Richards et al., 2021; Ladegaard-Pedersen et al., 2022; Sabatini et al., 2022; Esposito et al., 2023; Gigante et al., 2023; Romboni et al., 2023; Zaugg et al., 2023), bringing the total to n = 3096.

The coordinates of each sample served as the basis for the spatial distribution of isotopic ratios. In some few cases, the specific spatial coordinates of samples were not reported in the original publication, which provided only their distance from the archaeological site. In such instances, samples were assigned the coordinates of the reference site; the distance from the site reported by Authors never exceeded 7 km.

The newly added samples encompass various $^{87}Sr/^{86}Sr$ archives, which were categorised following Lugli et al. (2022) into distinct groups (Table 1; see S.M. .xlsx spreadsheet for the whole dataset).

Human samples (n = 873) come from n = 25 archaeological sites, and all the available individuals were included in the dataset, regardless of the "local" or "non-local" origin defined by the original contribution. The effect given by the inclusion of possible outliers (e.g., born elsewhere) in the final dataset is limited by data processing as outlined in section 2.3.1 and 2.3.2).

The geographical distribution of the samples is indicated in Fig. 2.

As 2123 samples derive from a considerably smaller number of sampling locations (n = 388), the dataset was organised into n = 388 groups based on the geographical coordinates of the sampling points (hereafter referred to as "same-coordinate groups"). Group sizes range from n = 2 to 107 samples per location.

2.2. Materials: sample selection and database for the test case-studies (Fermo and Monterenzio Vecchio)

Fermo (Early Iron Age: 9th-5th cent. BCE) is a single nucleated settlement, located in the Marche Region of Italy, with multiple necropolises in its immediate surroundings. It has been part of the discussion about the formation of protourban centers in Iron Age Italy, whose archaeological materials and funerary rituals, as well as the isotopic studies conducted so far (Esposito et al., 2023), both point to a significant external contribution in cultural traditions and/or population, likely from one or more areas inside Northern Latium, Tuscany, part of Umbria and of Emilia Romagna.

Data are derived from Esposito et al. (2023), where they are presented in a detailed way. They include the Sr isotopic analyses of 54 individuals, each represented by a single sample, either extracted from the petrous bone (for 23 cremated individuals) or from teeth (for 31

Table 1
Sample category groups and occurrence.

Sample category	N. samples	Bioavailable/Non-bioavailable
Rock	332	Non-bioavailable
Soil (leachate)	317	Bioavailable
Water	518	Bioavailable
Plants	406	Bioavailable
Fauna	343	Bioavailable
Shell	74	Bioavailable
Fossil	93	Non-bioavailable
Food	140	Bioavailable
Human	873	Bioavailable

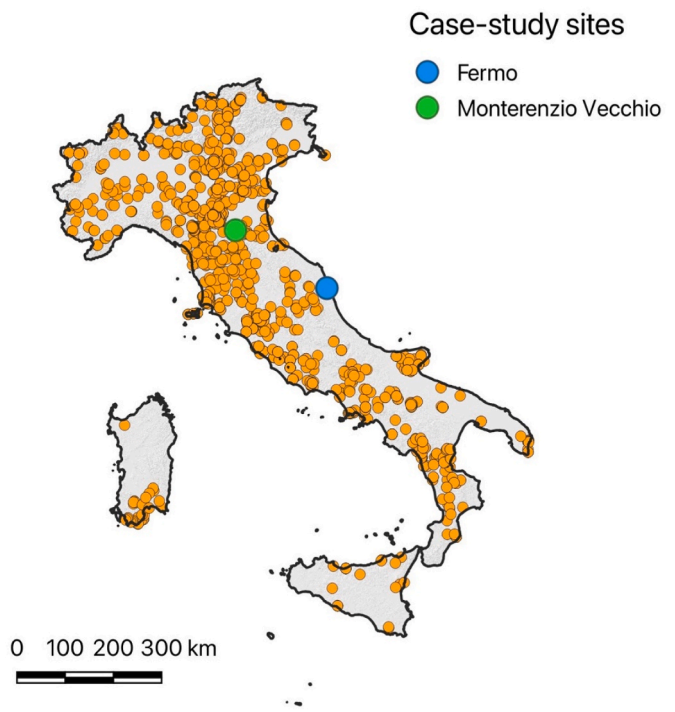

Fig. 2. Geographical distribution of bioavailable and non-bioavailable sample points across Italy (see Supplementary Material for complete dataset). The two sites used as case-studies are indicated on the map (light blue dot: Fermo; green dot: Monterenzio Vecchio). (For interpretation of the references to colour in this figure legend, the reader is referred to the Web version of this article.)

inhumed individuals), preferably from M1 (sampled for 26 out of the 31 inhumed individuals).

Monterenzio Vecchio (Late Iron Age: 4th-3rd cent. BCE) is a necropolis, whose precise reference settlement is unknown; it is related to the phase of the Celtic migrations to Italy, as recorded in the written sources, and shown by peculiar grave goods. Grave goods and skeletal non-metric dental traits, as well as the strontium isotopic ratios, have been used to investigate the possible origin and mobility of the buried individuals (Sorrentino et al., 2018). According to the Authors, this study highlighted "the migration of Celtic populations in Monterenzio as archaeologically hypothesized on the basis of the grave goods, followed by a high degree of cultural admixture between exogenous and endogenous traits".

Data are derived from Sorrentino et al., (2018), where they are presented in a detailed way. They include the Sr isotopic analyses of 23 inhumed individuals, most of which (21 out of 23) are represented by multiple samples, extracted from teeth. 21 individuals out of 23 had one M1 analysed. The multiple samples were used by the Authors to track the likely mobility of the individuals through their ageing, from infants to young adults.

A synthesis of the samples present in both case-study sites, listed by sampled material, is provided in Supplementary Material Table S7: it shows that, even if the samples are taken from different skeletal parts and their formation times don't precisely match, they anyway focus crucially on skeletal parts that form before birth or in the first years of life. As already stated (§ 1) the goal of the present paper is not to compare the mobility patterns between these two archaeological sites, but the two test cases have been selected to demonstrate the relevance of the method proposed here, also in terms of re-evaluation of former considerations. Another significant reason for our choice is that they were formerly investigated by some of the present Authors, and we could therefore have good control of the data, their problems and their implications.

The Fermo test case has been selected because its results are immediately relevant in terms of the discussion of the local baseline and the significant number of $^{87}Sr/^{86}Sr$ outliers allows to deploy the potential of the Unusualness index analysis.

The Monterenzio Vecchio test case has been selected particularly to monitor potential changes in local $^{87}Sr/^{86}Sr$ values from the isochrones to the original baseline, which was obtained using also pig tooth enamel data from a nearby site, and again for the discussion of the Unusualness index.

2.3. Methods

2.3.1. Data analysis: distribution analysis of bioavailable and non-bioavailable samples

Data analysis and subsequent processing were performed using the R project for statistical computing environment (R version 4.4.3, R Core Team, 2025) and QGIS (version 3.34.13-Prizren).

The Shapiro-Wilk Normality test was used to verify the normality of the sample distribution while the Kolmogorov-Smirnov test was used to compare different sample distributions between the two groups of data (e.g., bioavailable vs. non-bioavailable).

The percentage of outliers per category was assessed within each same-coordinate group, by using Tukey's IQR method. This was also represented in maps showing the geographical distribution of the IQRs and outlier percentages for each same-coordinate group (see Results section 3.2). The outliers were later eliminated from the groups, and median values for $^{87}Sr/^{86}Sr$ data were assigned to each group, thus minimising the presence of outliers and humans with a non-local origin.

Finally, the interpolation of data through Ordinary Kriging was carried out with R (see Supplementary Material Text S1, Supplementary Material Figs. S7, S8, S9, S10), and the Kriging models were imported into QGIS to finalise the maps.

2.3.2. Isochrones and Unusualness index

The case studies of Fermo (Early Iron Age) and Monterenzio Vecchio (Late Iron Age) were analysed by employing isochrones and the Unusualness index (see below for details). As anticipated in the introduction, the two case studies represent a real-data application that serve a dual purpose: (1) to assess the strengths and limitations of isoscapes in provenance studies and (2) to introduce a more nuanced mobility framework using isochrones and statistical methods.

Isochrones, defined as lines enclosing areas reachable within specific timeframes, were employed to model site catchment areas. These correspond to least-cost site catchments (LCSC), representing regions accessible within a defined cost threshold, here measured as walking time (Herzog, 2020). The Digital Elevation Model of Italy (TINITALY/1.1) (Tarquini et al., 2023) and site coordinates were used to generate the isochrones. For both sites, walking areas were calculated up to 1 h, between 1 and 2 h, and between 2 and 10 h. The first isochrone (1 h, equivalent to a 2h round trip) is assumed to represent strictly local movements, thereby forming a restricted baseline. The second isochrone (2 h, or 4h round trip) captures short-term movements typical of subsistence mobility (Gregoricka, 2021). The third isochrone (10 h, or 20h round trip — ca. day long mobility) encompasses longer one-way journeys, reflecting more complex mobility with potential social or economic implications, such as shifts in residence (Gregoricka, 2021). From this perspective, the third isochrone (10 h walking time) could represent a threshold given here to the concept of autochthony for the two Early and Late Iron Age sites. It should be noted that the mobility categories presented here are not fixed and can be adapted to suit the archaeological context under study. Pedestrian travel is prioritised for modelling because it provides a conservative, uniform, replicable and well-constrained reference, adopted since the beginnings of Site-Catchment Analysis (Vita-Finzi et al., 1970). In the Iron Age of Italy, the provenance of food from more distant sources, or a wider mobility of

animals for seasonal feeding is possible, but, particularly before the Archaic Age, for the Fermo case, the main food sources are expected to come from the constrained territories of nucleated settlements (Motta, Beydler, 2021). Other mobility modes can be highly variable and cannot be parameterised reliably without strong assumptions. The Monterenzio Vecchio case could possibly involve a higher degree of staple trade, as local communities in the late Iron Age are seen as rural settlements trading with major nucleated settlements; but their local farming economy could be scarcely influenced by imported products (Ortalli, 1990). In any case, the walking-based isochrone adopted here reduces the risk of over-estimating catchments.

The elaboration of the isochrones was achieved using the "r.walk" function in Grass, available in QGIS, which produces a raster map for each site, showing the anisotropic cumulative cost associated with movement. This algorithm utilises the Langmuir model (Langmuir, 1984). The raster was reclassified into three value classes: value 1 includes raster cells with values less than or equal to 3600 s; value 2 includes cells between 3600 and 7200 s; value 3 includes cells with values greater than 7200 s, but less than 60,000 s. These classes were defined based on the time intervals used for the isochrones. $^{87}Sr/^{86}Sr$ values from the isoscape raster were extracted from the polygons corresponding to the three isochrone classes to enable a comparison with the human $^{87}Sr/^{86}Sr$ values.

To compare human sample $^{87}Sr/^{86}Sr$ ratios with isochrone values, the Unusualness index was employed, which measures how each individual's $^{87}Sr/^{86}Sr$ value deviates from the median values within the three isochrone levels. This allows to estimate the difference between human samples and the isotopic landscape contained in the isochrones, by associating an Unusualness index (UN) value to each individual in the test set, calculated according to the following formula (Drennan, 2009):

$$UN = \frac{SrCx - MdIsoc}{MdSpIsoc}$$

where "SrCx" = $^{87}Sr/^{86}Sr$ value of the individual sample; MdIsoc = Median of the Isoscape $^{87}Sr/^{86}Sr$ values within the isochrones relative to the site of sample "Cx"; MdSpIsoc = Interquartile range of $^{87}Sr/^{86}Sr$ isochrones values around the site of sample "Cx".

To adopt a more nuanced approach in this analysis, varying degrees of Unusualness were considered in relation to all three isochrones combined, reflecting different scales of mobility, which can represent the shift between the place of birth (or growth) of individuals and the place of interment, and not life-long mobility.

The relationship between $^{87}Sr/^{86}Sr$ values of human samples and those of the surrounding landscape was scored according to the Unusualness index. Stemming from the Unusualness scores on the 10 h isochrones, we recognise 3 classes of mobility, defined here as *stable, circadian mobility* and *long-range mobility*. The first class is composed of individuals placed within an Unusualness score range of $-1 \leq UN \leq +1$, the second of those falling between $+1 < UN \leq +3$ or $-1 > UN \geq -3$, while the third encompasses individuals which fall outside said intervals, both in a negative or positive direction. This approach is grounded in the argument that mobility, as a phenomenon, transcends the rigid dualism of "local" versus "non-local", a dichotomy often narrowly defined by a limited radius around the site of discovery. The Unusualness score could potentially vary from -inf to +inf. The individuals who deviate from the Zero value and display an Unusualness index higher than the absolute value of 3, are here considered as non-local to the area represented by the isochrones.

While the thresholds of ±1 and ±3 are partly arbitrary, their selection is supported by Tchebichef 's inequality theorem, which states that in any distribution, at least 75% of the data falls within 2σ of the mean, while at least 89% lies within 3σ (Tchebichef, 1867; DeGroot and Schervish, 2012). Although the theorem does not establish a specific rule for ±1σ, this threshold serves as a practical way to define "usual" values, representing samples that are close to the median and within the expected local range.

Despite the Unusualness index relying on the interquartile range (IQR) rather than standard deviation, the underlying principle remains consistent. The ±1 threshold marks the interval in which data points are closest to the median, while the ±3 threshold defines a boundary beyond which fewer than ~11% of data points are expected to fall, indicating a deviation from the main distribution.

By employing a consistent scale to quantify "isotopic deviation", this approach enhances our understanding of the relationship between individual samples and the surrounding landscape, extending up to 10 h of walking distance from the site.

Furthermore, the values for individual samples vary within this range, leading to an individual assessment of mobility. It should be noted that this method is applicable when geographical relocation led to a shift in the isotopic signature assimilated through the diet of the analysed individuals. For this reason, to achieve full effectiveness, these steps should ideally be used with LA (laser ablation) sampling on teeth and other tissues, as they provide greater precision in defining mobility and are not affected by the averaging of varying $^{87}Sr/^{86}Sr$ values related either to multiple individual movements or an incomplete equilibration with the Sr body pool (see e.g., Nava et al., 2020; Lugli et al., 2022).

To compare the classifications proposed in this study with those presented in the original publications, a mismatch percentage was also calculated (Supplementary Material Table S6). For this purpose, the current ternary classification (stable, circadian mobility and long-range mobility) was converted into a binary one using two alternative methods: 1. Treating the circadian mobility category as local; 2. Treating the circadian mobility category as non-local. Additionally, individuals originally defined in former publications as possible or probable locals/non-locals were treated as certain.

3. Results

3.1. Data analysis: distribution analysis of bioavailable and non-bioavailable samples

As expected, the initial distribution analysis of all samples —carried out to examine the general statistical parameters— indicated a sample distribution deviating from normality (Shapiro-Wilk Normality test, $W = 0.46$, p value < 0.001) (see Supplementary Material Figs. S1 and S2).

The distinction made between bioavailable and non-bioavailable samples (see Supplementary Material Figs. S3 and S4) identified greater variability within the non-bioavailable dataset, consisting of rocks and fossils, despite its smaller sample size. This contrasted significantly with bioavailable samples (Kolmogorov-Smirnov Test, $D = 0.29$, p value < 0.001, see Supplementary Material Fig. S4). By examining specific sample categories across the whole of Italy (see Supplementary Material Fig. S5), it became apparent that some of these stood out for their variability. This is evident for rock and water samples, which are highly variable, and for fossils, which conversely present a very narrow range with less radiogenic (i.e., lower) values. Human data variability fits within the ranges relative to other bioavailable sample categories (see Supplementary Material Fig. S5).

The analysis of same-coordinate groups (n = 388 unique groups with more than 2 samples each) included the assessment of their outlier percentage (Fig. 3) which varies among groups from 0% to 11.1%: despite the large number of human samples (n = 873), only 7% were classified as outliers. This trend remained consistent across most categories, with generally low outlier percentages (e.g. plants, soil, water). Notably, small mammals exhibited a slightly higher outlier rate (8%), while shells showed an increased percentage (11.1%), reinforcing existing concerns about their reliability (Yanes et al., 2008; Maurer et al., 2012; Lugli et al., 2022; Esposito et al., 2023). Regarding rocks and fossils, their shape of distribution combined with their mostly non-bioavailable nature (see Supplementary Material Figs. S4 and S5)

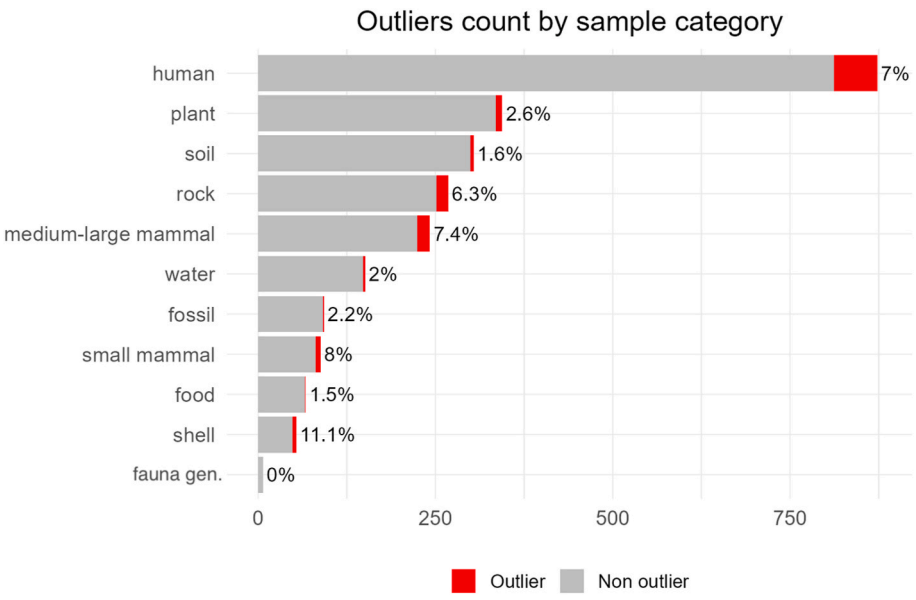

Fig. 3. Bar chart representing the total number of samples for each sample category (same-coordinate groups) and the outlier percentage (red). (For interpretation of the references to colour in this figure legend, the reader is referred to the Web version of this article.)

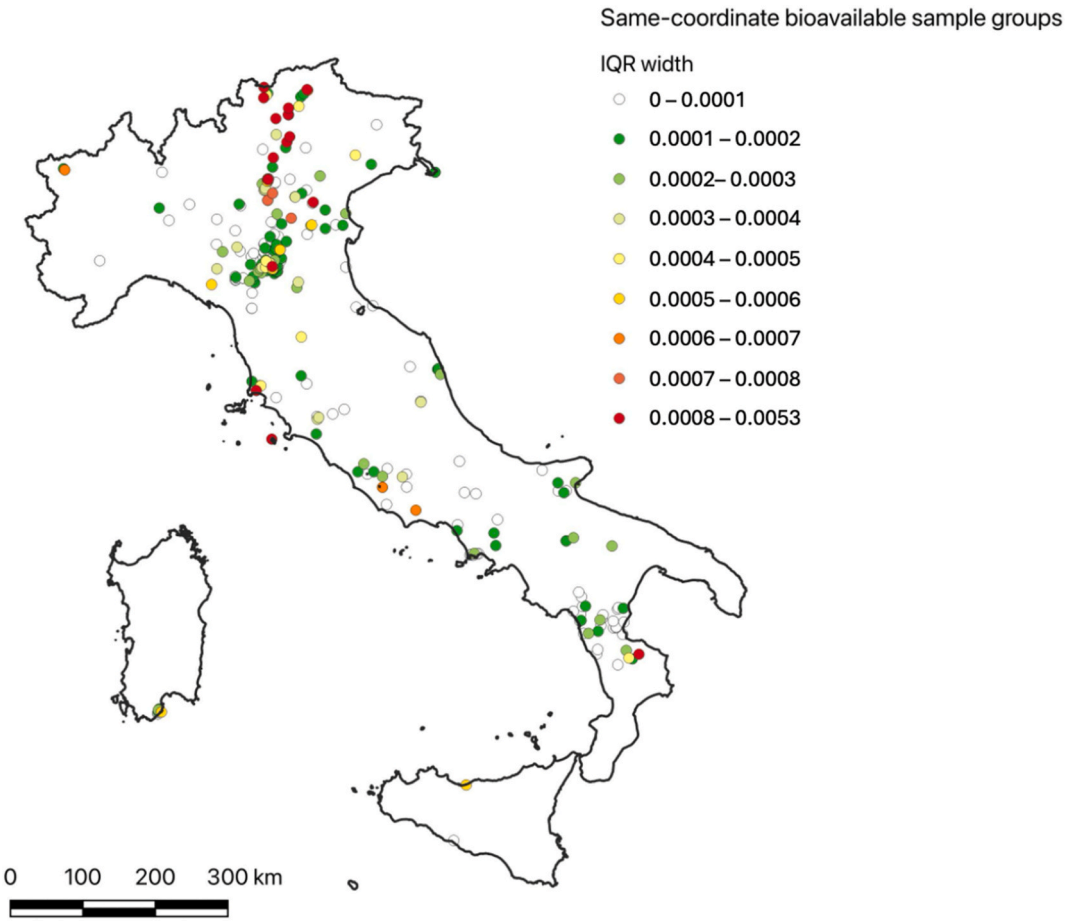

Fig. 4. Same-coordinate based bioavailable sample groups represented according to their IQR width. (For interpretation of the references to colour in this figure legend, the reader is referred to the Web version of this article.)

has led to their exclusion from further analysis, focusing instead on the bioavailable sample categories for data processing and Kriging.

3.2. Bioavailable samples in same-coordinate groups and datasets used

Bioavailable sample groups' IQRs tend to be greater in northern Italy (Fig. 4). This was most prominent in Trentino-Südtirol and Veneto, suggesting a correlation with the articulated geological settings of those regions.

The outlier percentage map (Supplementary Material Fig. S6) highlights clustering in the Pianura Padana region and along the Apennine chain, likely influenced by higher sampling density in the former and by the presence of a pool of sediments from diverse Alpine and Apennine (and Po Plain) sources in both areas. Some same-coordinate groups displayed outlier rates as high as 28–40%, mainly observed in Northern and Central Italy.

The most variable groups, in terms of IQR width, are associated with human and faunal samples (both small and medium-large mammals). This was expected, as groups of human samples may include non-local individuals, while medium-to-large mammals (e.g., *Bos* and *Sus*) also frequently exhibit mobility-related isotopic variation (Trentacoste et al., 2020; Dávila et al., 2024). Additionally, the fact that most of these faunal samples consist of bone tissue (n = 337) is significant. Diagenetic processes tend to alter the $^{87}Sr/^{86}Sr$ ratios in bone to align with the surrounding soil, but incomplete alignment may result in mixed values that fall between the original tissue and the local sediment ratio (Nelson et al., 1986; Sillen and Sealy, 1995; Hedges, 2002; Trickett et al., 2003; Bentley, 2006; Lee-Thorp and Sealy, 2008). As anticipated in section 2.3.1, outlying samples from any bioavailable category, identified through Tukey's IQR method, were removed from the dataset, and the median value was calculated for each same-coordinate group. Samples with unique coordinates were directly included in the dataset. A distinction was made between datasets: in one case, an "All Bioavailable Samples" (ABS) dataset was built, encompassing all bioavailable sample categories. In the other, a more conservative approach was employed, excluding all human and medium-to-large mammal samples from the dataset. This was thereby named "Selected Bioavailable Samples" (SBS) dataset and was created with the aim of evaluating the impact of the excluded sample categories, as these were largely responsible for increased IQR width and outlier percentages in many same-coordinate groups and are likely to exhibit mobility or variable feeding regimes (Holt et al., 2021; Wright, 2005). As indicated in Fig. 5, however, variability remained present even after these steps, particularly in correspondence of geologically diverse regions, such as the Alpine arc, where variable $^{87}Sr/^{86}Sr$ end-members are existent.

3.3. Ordinary Kriging

The final output results in two distinct isoscapes (ABS and SBS) generated with Ordinary Kriging on a 1×1 km cell size, and their associated error maps (Fig. 6A, B, 7A, B). No visually appreciable differences were noted between the two isotopic maps (Table 2).

The two isoscapes revealed that most of Italy is generally covered by low prediction error (Fig. 6B and Fig. 7B), except, as expected, for areas where samples are too sparse.

3.4. Kriging comparison: All Bioavailable Samples (ABS) vs. Selected Bioavailable Samples (SBS) isoscapes

By comparing the Root Mean Square Error (RMSE) and R^2 values (Table 3), no appreciable changes were noticed between the two isoscapes. In fact, the R and adjusted R^2 values (Supplementary Material Fig. S11) indicate there is close to no difference between the two isoscapes. This is visible in the map in Fig. 8, and in the scatter plot in Supplementary Material Fig. S11. While RMSE is not always the best measure for evaluating isoscape accuracy (Holt et al., 2025), it remains valid for comparing two Kriging-based isoscapes of the same region.

The areas most sensitive to the presence of humans and medium-to-large mammals in the dataset are the Northern regions of Italy, where dark red patches are visible. Other positive variations, though slight, are also visible in central Italy, Sicily and Apulia. In addition to this analysis, two comparison maps were generated, including the isoscapes and the bioavailable Ordinary Kriging map produced by Lugli et al., in 2022 (see Supplementary Material Fig. S12A and S12B; Supplementary Material Text S2), along with their corresponding scatter plots (see Supplementary Material Figs. S13 and S14).

Finally, the ABS–SBS Kriging comparison guided the decision to adopt the ABS isoscape for the case-study applications, which anyway does not differ substantially from the SBS. In addition, constructing the isoscape from all bioavailable data —ABS: including human and mammalian samples— prevents attenuation of the bioavailable signal; their inclusion, together with robust distributional summaries (e.g., Tukey's IQR and the median for each set of coordinates), minimises the influence of outliers and improves isoscape robustness.

3.5. Test case studies: isochrones and Unusualness index

Both case studies concern sites dating to the Iron Age, a period in Italian protohistory in which territoriality is considered a defining feature.

3.5.1. Fermo (Marche, 9th-5th century BCE)

Fermo was chosen as it represents a site with archaeological and historical importance, where archaeological materials and funerary rituals, and isotopic studies conducted so far (Esposito et al., 2023), point to a significant external contribution in cultural traditions and/or population. In fact, it is considered a site with strong connections with the Villanovan groups of Tyrrhenian Etruria and Northern Italy in the area of Bologna (a "Villanovan-influenced site"), within the territory characterised by the material culture associated with the "Picene" Adriatic groups, in the context of the Italian Early Iron Age (Lollini, 1976; Pallottino, 1984; Torelli, 1986).

The overall $^{87}Sr/^{86}Sr$ range derived from the totality of the three isochrones, traced on the ABS isoscape (Fig. 9, Table 4), corresponds to 0.7085-0.7090. The local ABS data component encompasses local (according to Tukey's IQR) human samples, fauna (*Sus scrofa* and *Ovis vel Capra*), water and soil.

The first and second isochrones have a very limited and similar range (1 h isochrone: 0.7089-0.7090; 2 h isochrone: 0.7089-0.7090; values are rounded to 4 decimal places for readability, Table 4 reports values to 5 decimal places), while the third covers a wider range of lower $^{87}Sr/^{86}Sr$ values (10 h isochrone: 0.7085-0.7090). The human samples' lower $^{87}Sr/^{86}Sr$ values are mostly included in the three isochrones, while the more radiogenic ones are not.

The Unusualness index was applied to examine the relationship between individual human isotopic signatures and those of all three isochrones (10 h). Fig. 10 shows the density distribution of the Unusualness index calculated for the 10 h isochrones. According to the definition previously given (see Methods section 2.3.2), we identify here n = 39 stable individuals (72% of the total), n = 11 individuals subject to circadian mobility (20%) and n = 4 to long-range mobility (8%), (see Supplementary Material Tables S1 and S3 for sample IDs, Unusualness scores and comparison with the original study's results).

3.5.2. Monterenzio Vecchio (Emilia-Romagna, 4th – 3rd century BCE)

The Second Iron Age necropolis of Monterenzio Vecchio displays cultural syncretism between incoming Celtic populations and indigenous Etruscan ones, as evidenced by its funerary practices, and was originally analysed by Sorrentino et al., in 2018. This case study was selected to monitor potential changes in local $^{87}Sr/^{86}Sr$ values from the isochrones to the original baseline. The latter was built upon pig tooth enamel from the coeval site of Pianella di Monte Savino (Scheeres et al.,

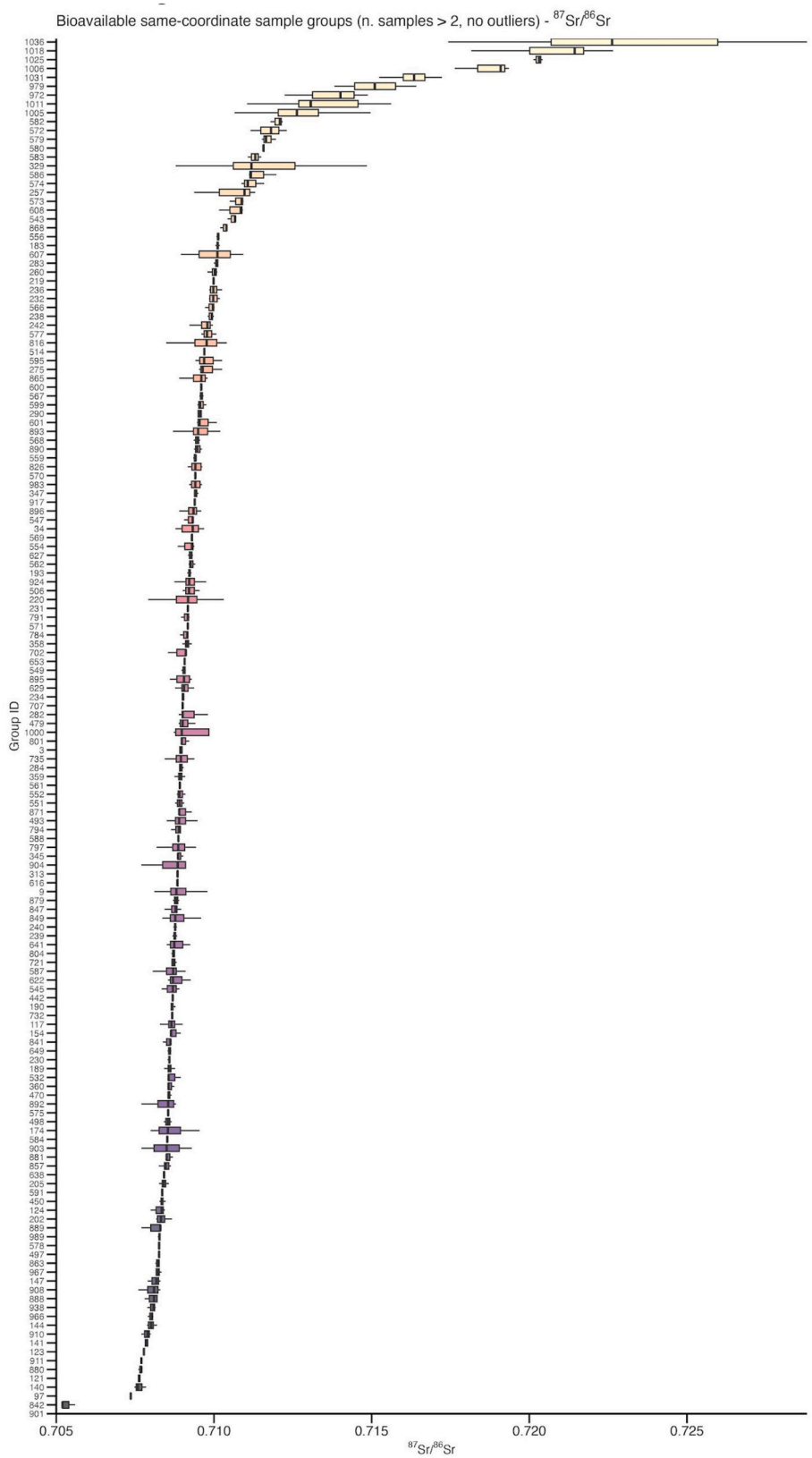

Fig. 5. Box and whisker plots depicting the $^{87}Sr/^{86}Sr$ range of bioavailable, same-coordinate based sample groups within the ABS dataset (number of samples >2 for the same location) after the elimination of outlying samples through Tukey's IQR method. The box and whisker plots are ordered according to their increasing $^{87}Sr/^{86}Sr$ median values.

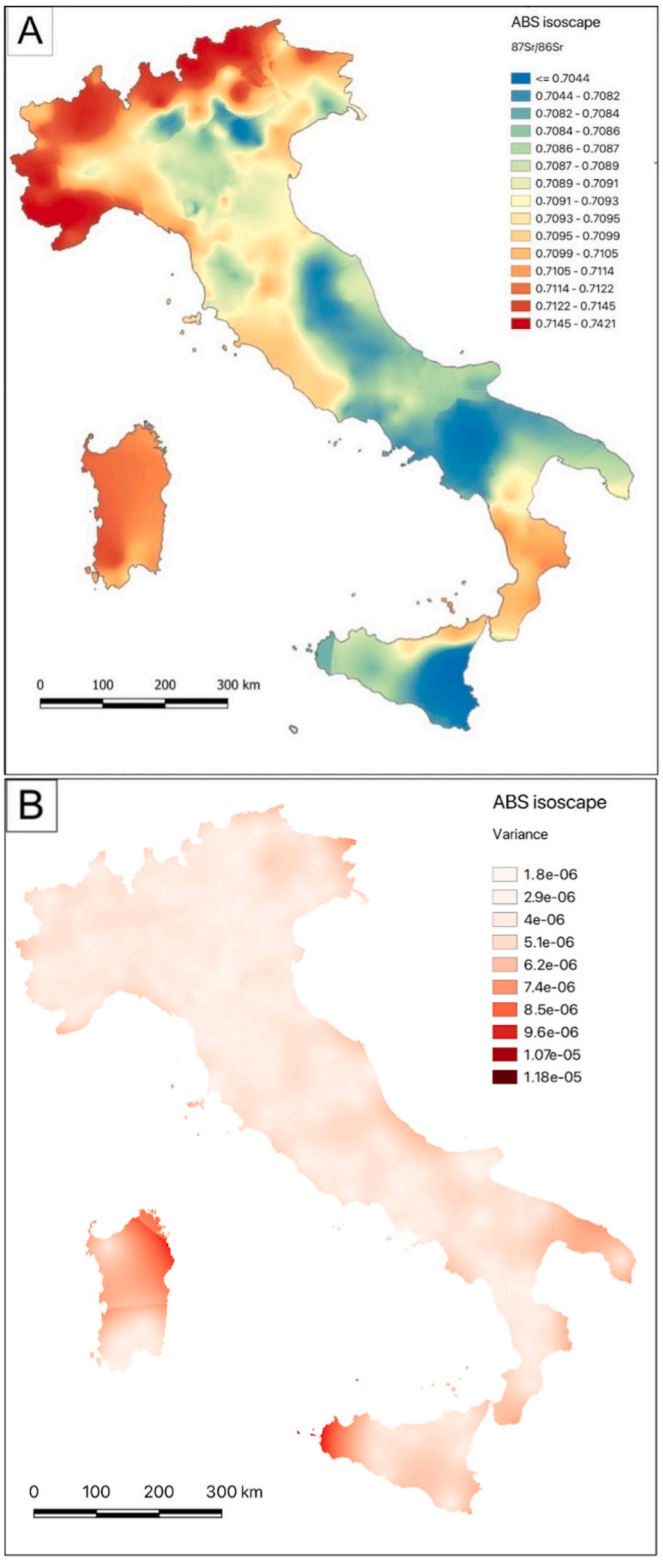

Fig. 6. All Bioavailable Samples isoscape: A. Ordinary Kriging map (cell size = 1000 × 1000 m); B. Error map (prediction variance, cell size = 1000 × 1000 m). The maps are also available as.tif in the Supplementary Materials. (For interpretation of the references to colour in this figure legend, the reader is referred to the Web version of this article.)

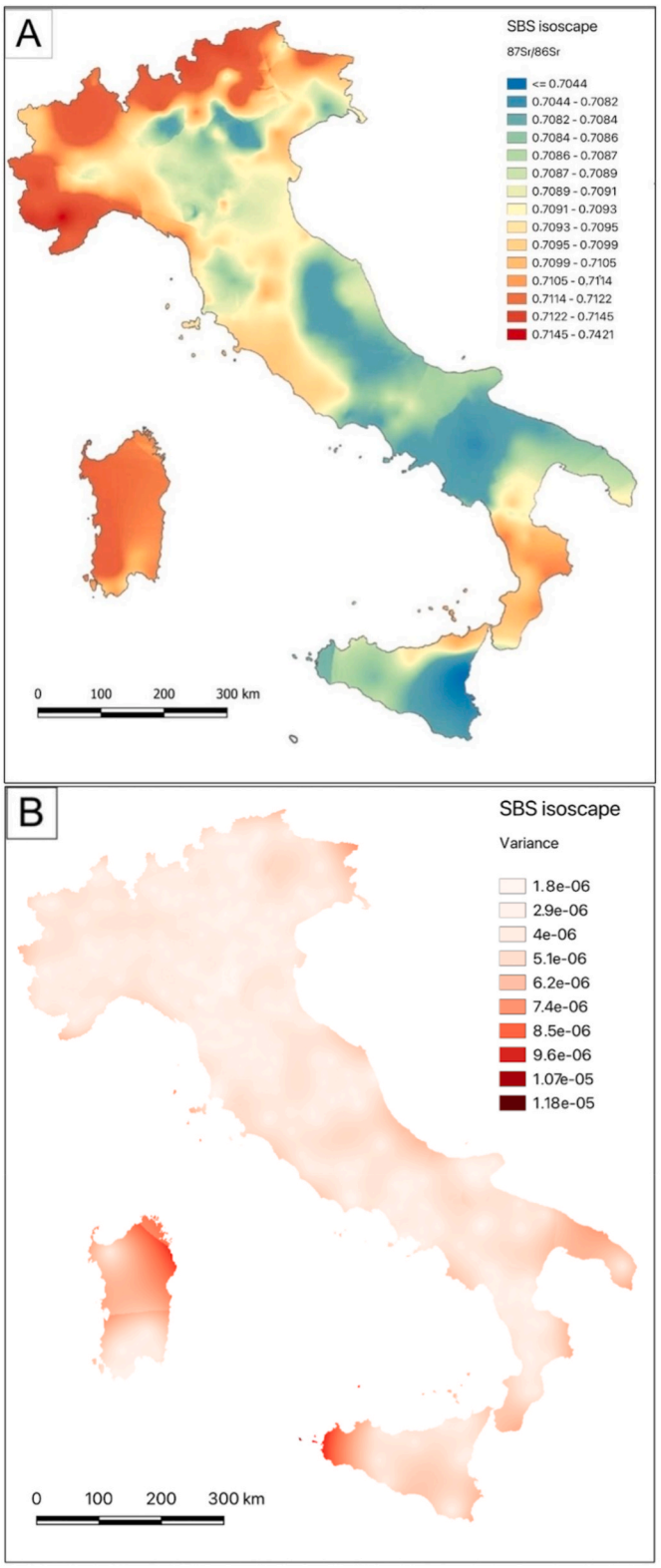

Fig. 7. Selected Bioavailable Samples isoscape: A. Ordinary Kriging map (cell size = 1000 × 1000 m); B. Error map (prediction variance, cell size = 1000 × 1000 m). The maps are also available as.tif in the Supplementary Materials. (For interpretation of the references to colour in this figure legend, the reader is referred to the Web version of this article.)

Table 2
Summary statistics of the **All Bioavailable Samples** Isoscape and **Selected Bioavailable Samples** Isoscape.

	All Bioavailable Samples Isoscape (ABS)	Selected Bioavailable Samples Isoscape (SBS)
Median	0.7091	0.7092
Mean	0.7101	0.7101
SD	0.0029	0.0029

Table 3
RMSE and R^2 comparison between the All Bioavailable Samples (ABS) isoscape and the Selected Bioavailable Samples (SBS) isoscape (10-fold Cross-Validation).

	RMSE	R^2
ABS	0.00269	0.50
SBS	0.00271	0.50

2013), located ca. 5 km from Monterenzio Vecchio, where instead human bone samples were collected (Sorrentino et al., 2018). The $^{87}Sr/^{86}Sr$ values of the pig teeth and human bone samples do not coincide, but are very similar —a discrepancy attributed by the authors to potential diagenetic effects, though it may also reflect the differing geological settings of the sites. These samples were nevertheless included in the initial dataset and processed according to the methods outlined in sections 2.3 and 3.4.

The overall $^{87}Sr/^{86}Sr$ range displayed by the three isochrones traced on the ABS isoscape (Fig. 11, Table 5) corresponds to 0.7088-0.7093.

As seen in Fig. 11, the first and second isochrones have a limited range with similar values (1 h isochrone: 0.7089-0.7090; 2 h isochrone: 0.7089-0.7090), while the third covers a wider range of higher $^{87}Sr/^{86}Sr$ values (10 h isochrone: 0.7088-0.7093).

By applying the Unusualness index on all three isochrones (Fig. 12), however, a more nuanced vision of mobility emerges: considering the 10 h isochrones, it was possible to identify n = 13 (30%) as stable, n = 22 (50%) as circadian mobility and n = 9 (20%) as long-range mobility samples (see Supplementary Material Tables S2 and S4 for sample IDs,

Table 4
General statistics of isochrones (ABS isoscape) of Fermo.

ABS isoscape			
	1 h	2 h	10 h
min Sr	0.70891	0.70893	0.70851
median Sr	0.70893	0.70893	0.70886
max Sr	0.70896	0.70900	0.70899

Unusualness scores and comparison with the original study's results). It should be noted that the human dataset from Monterenzio comprises double sampling for almost every individual (e.g., two different teeth), used by the authors to interpret the results as evidence of mobility either towards or away from the site. Similarly, our analysis shows that, in some cases, both samples from the same individual fall within the same mobility class, while in others they fall into different categories (e.g., stable in one sample and circadian in the other), depending on the mineralised tissue analysed. The results indicate a significant degree of mobility, mainly involving displacements away from the site during infancy or early adolescence.

4. Discussion

The evaluation of isoscapes, sample category inclusion, and mobility assessment methods in this study has identified key issues while also proposing possible solutions. Non-bioavailable samples exhibit extreme variability and rarely align with the distribution of bioavailable $^{87}Sr/^{86}Sr$ proxies, complicating their integration into Ordinary Kriging isotopic maps. Among bioavailable samples, plants and soil have proved to be the least deviating $^{87}Sr/^{86}Sr$ proxies, whereas water, snail shells, bones and teeth of humans and fauna (encompassing small and medium-large mammals) show more significant variability. Moreover, bone tissue is prone to diagenesis effects, making its use less suitable for mobility studies, unless precautionary steps are taken (Nelson et al., 1986; Sillen and Sealy, 1995; Hedges, 2002; Trickett et al., 2003; Bentley, 2006; Lee-Thorp and Sealy, 2008). Data processing —such as Tukey's IQR method and the assignment of median values to same-coordinate groups— is crucial for the building of $^{87}Sr/^{86}Sr$ prediction maps, as it

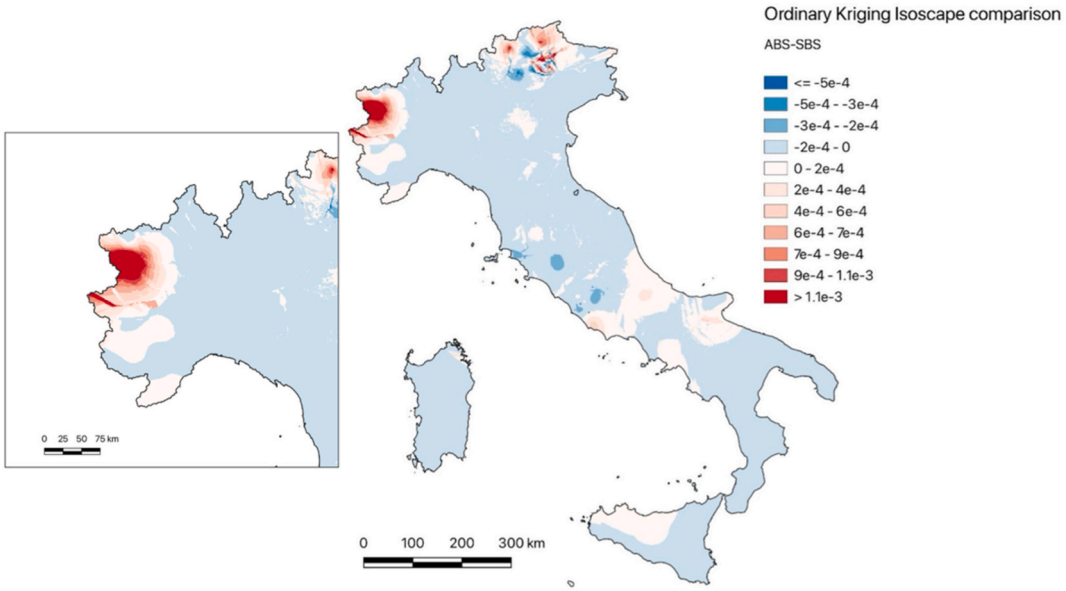

Fig. 8. Variation map depicting the difference in prediction between the two isoscapes, created by subtracting the SBS raster from the ABS one. Patches within the blue scale indicate areas where the ABS isoscape exhibits lower values than that of the SBS (negative difference), white patches signal areas where variations are close to none. Red scale areas indicate increasingly higher values in the ABS isoscape (positive difference). (For interpretation of the references to colour in this figure legend, the reader is referred to the Web version of this article.)

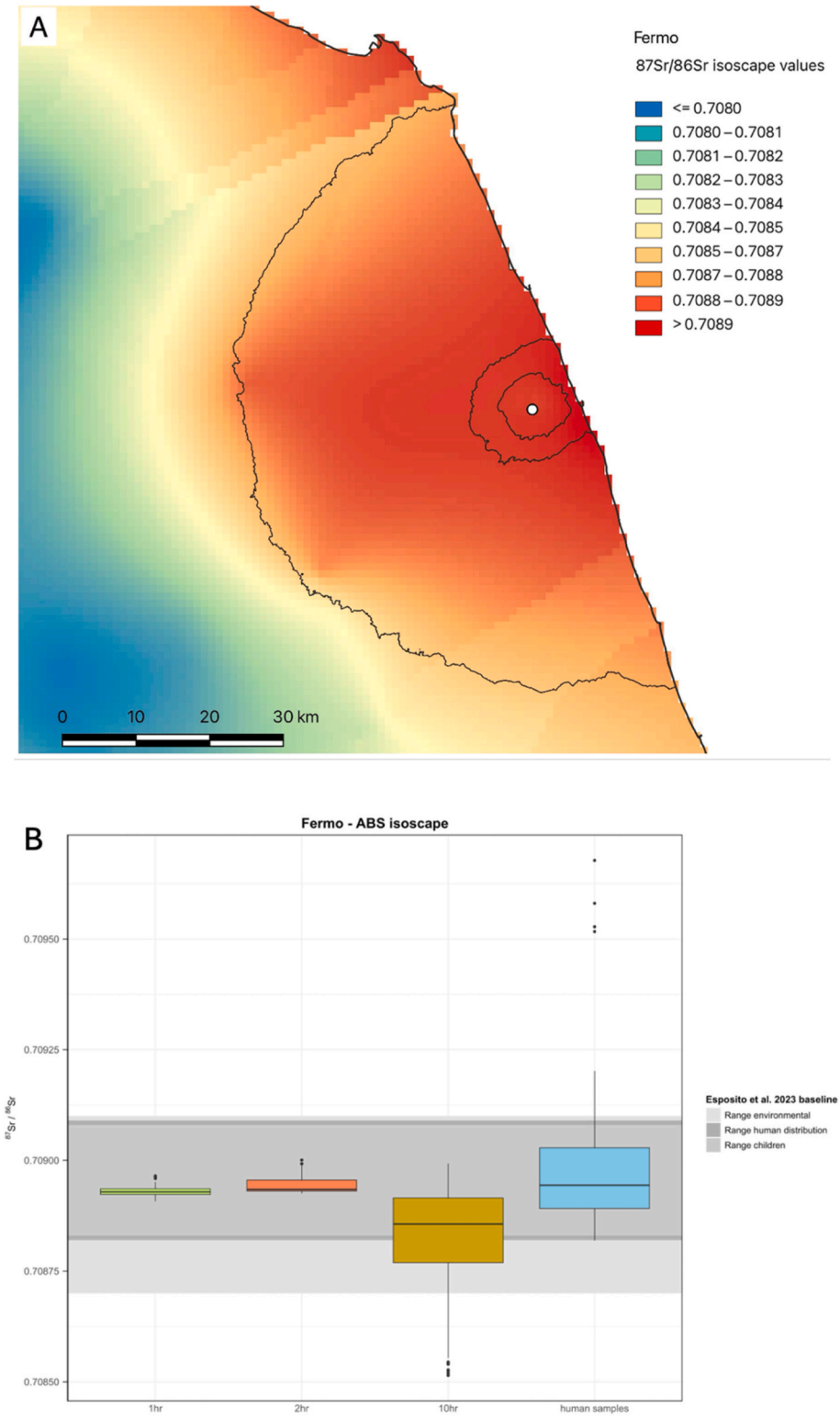

Fig. 9. A. $^{87}Sr/^{86}Sr$ values within the isochrones (black lines) around Fermo superimposed on the ABS isoscape (See Supplementary Material Fig. S15 for the distribution of bioavailable sample units within the isochrones); B. $^{87}Sr/^{86}Sr$ box and whisker plots representing 1, 2, 10 hour isochrones and human samples superimposed over the original baseline values (Esposito et al., 2023). (For interpretation of the references to colour in this figure legend, the reader is referred to the Web version of this article.)

allows to exclude biased or anomalous samples, while including useful sample categories (i.e., humans and medium-to-large mammals). Excessive variability complicates Kriging-based interpolation, leading to the adjustment of variogram (VGM) models to fit. Inadequate sampling in areas such as the Adriatic coast, the Alpine arc and the major islands further affects the interpolation's consistency. While efforts to address

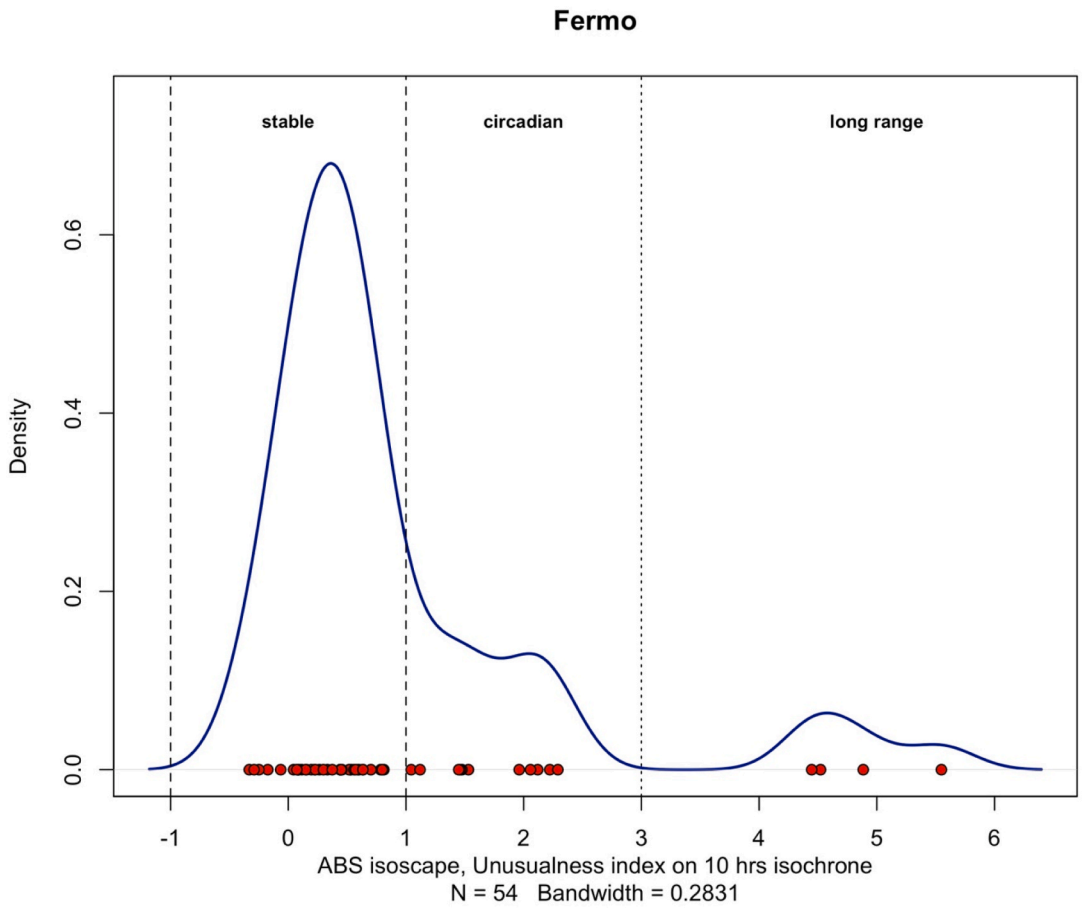

Fig. 10. Fermo's Unusualness index (10 h) density plot, depicting the relationship between human samples (red dots) and the All Bioavailable Samples (ABS) isoscape isochrones. Points between $-1 \leq UN \leq +1$ are regarded as stable, those falling between $+1<UN \leq +3$ and $-1>UN \geq -3$ as circadian mobility individuals, while values outside the +3 and −3 range are considered long-range mobility individuals. (For interpretation of the references to colour in this figure legend, the reader is referred to the Web version of this article.)

Table 5
General statistics of isochrones (ABS isoscape) of Monterenzio Vecchio.

ABS isoscape			
	1 h	2 h	10 h
min Sr	0.7089	0.7089	0.7088
median Sr	0.7089	0.7089	0.7090
max Sr	0.7090	0.7090	0.7093

these gaps have begun —such as Ladegaard-Pedersen et al. (2022) work in Lake Garda, Gigante et al.'s (2023) Sardinia isoscape, Zaugg et al.'s (2023) Sybaris region study and Defant et al.'s (2025) isoscape of Liguria— more evenly distributed sampling is needed. Randomised, wide-scale sampling could mitigate current biases, improving Kriging accuracy (Rossi et al., 2024). Prioritising less variable sample categories, such as plants, while cautiously integrating more variable sources, could further enhance prediction precision. A clear trend is visible within the ABS and SBS isoscapes (see Supplementary Material Figs. S9 and S10), consisting in an underestimation of higher $^{87}Sr/^{86}Sr$ values. This likely results from a low number of datapoints in areas with high $^{87}Sr/^{86}Sr$ values, along with less homogeneous spatial coverage.

Finally, the ABS (All Bioavailable Samples) isoscape was chosen as its dataset encompasses a wider number of samples, including human and animal $^{87}Sr/^{86}Sr$ variability. The risk of including non-local individuals is minimised by the elimination of outliers through Tukey's IQR method and by the assignment of median values within the same-coordinate groups. For these reasons, a more inclusive dataset was deemed best-fitting.

Regarding the use of isochrones and the Unusualness index, these have proved to be especially useful in the application of a more nuanced approach to mobility. Isochrones allow for the investigation of $^{87}Sr/^{86}Sr$ values present in different areas of the landscape around a given site, with the advantage of also taking into consideration its morphology and potential connectivity. The extraction of $^{87}Sr/^{86}Sr$ values from each pixel within the isoscape raster involves both risks and benefits. The main risk consists in potentially encountering areas with high prediction error, opposed to the major benefit of considering the $^{87}Sr/^{86}Sr$ values of a wider area in the assessment of mobility, thus overcoming the limit of spatially restricted $^{87}Sr/^{86}Sr$ baselines, with ranges usually confined to a few km around a site. If used carefully, this method allows a useful spatial expansion of the investigated area. Regarding the Unusualness index calculated on human and isochrone $^{87}Sr/^{86}Sr$ values, the application to each case-study presented here has confirmed its usefulness in returning a gradual dimension of the relationship occurring between individuals and the surrounding isotopic landscape. This method also has the advantage of making results comparable by positioning each sample on a scale. The combination of isoscapes, isochrones and Unusualness index has its strengths in the overcoming of comparisons between anthropological samples' values to those given by a limited amount of baseline samples, generally referring to a site's proximity. The issue of these traditional "exclusion" (local vs. non-local) methods, usually employing standard crow-flight buffer zones around a site, is the over-simplification of the relationship between human bulk $^{87}Sr/^{86}Sr$

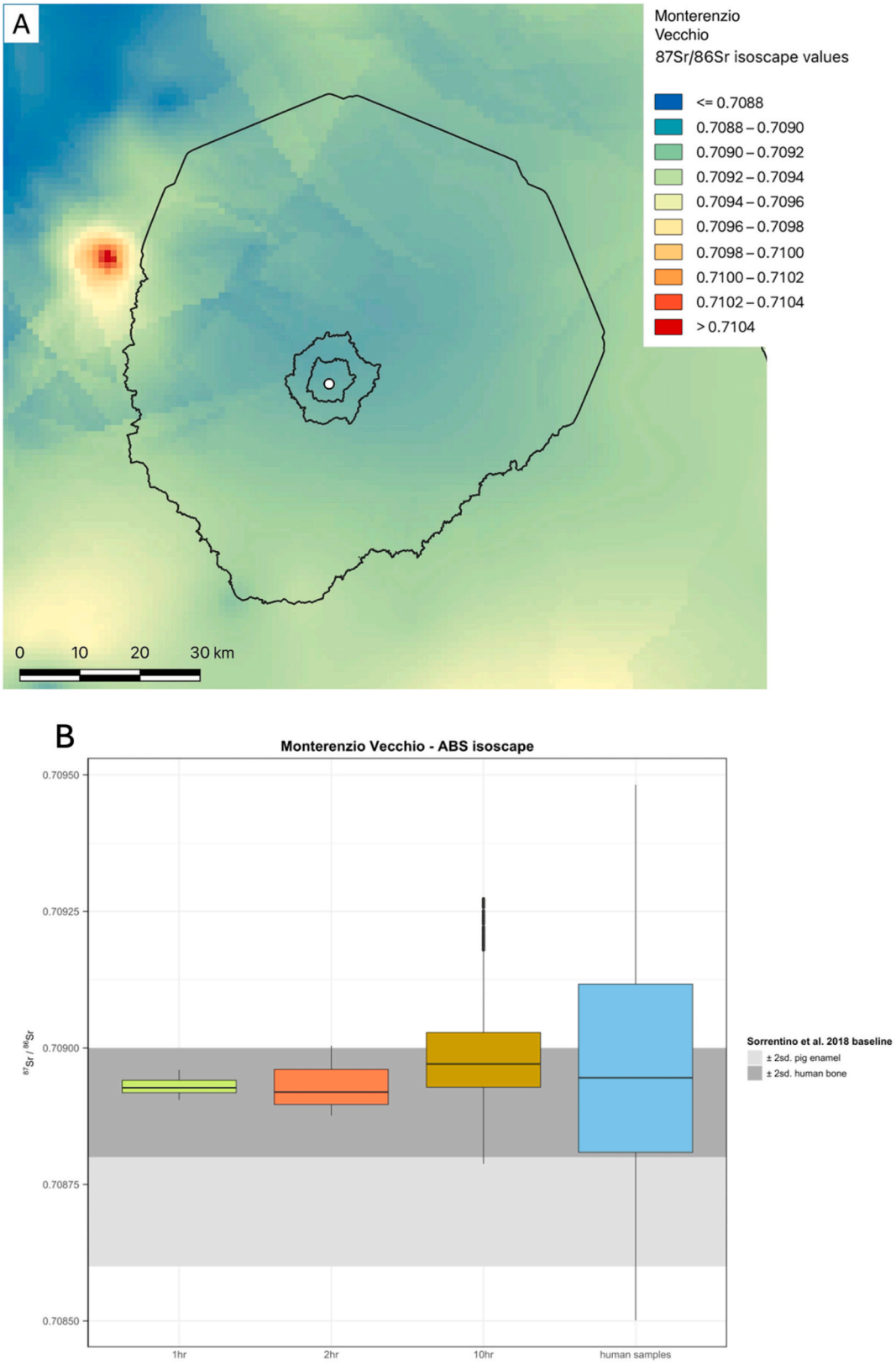

Fig. 11. A. $^{87}Sr/^{86}Sr$ values within the isochrones (black lines) around Monterenzio Vecchio superimposed on the ABS isoscape (See Supplementary Material Fig. S16 for the distribution of bioavailable sample units within the isochrones); B. $^{87}Sr/^{86}Sr$ box and whisker plots representing 1, 2, 10 h isochrones and human samples superimposed over the original baseline values (Sorrentino et al., 2018). (For interpretation of the references to colour in this figure legend, the reader is referred to the Web version of this article.)

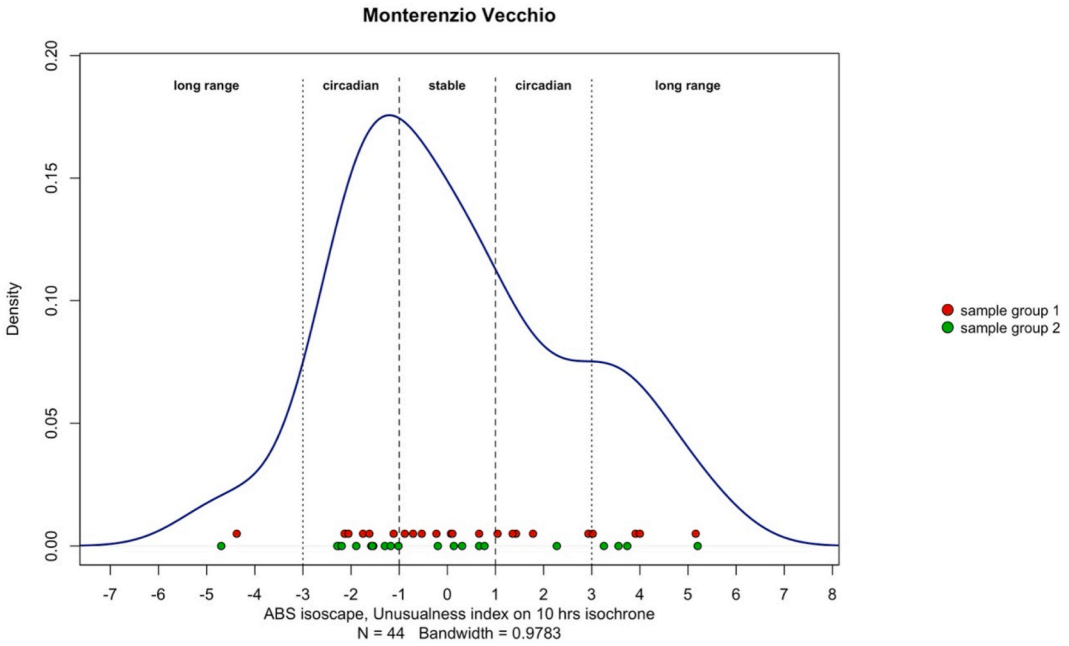

Fig. 12. Monterenzio Vecchio's Unusualness (10 h) index density plot, depicting the relationship between human samples and the All Bioavailable Samples (ABS) isoscape isochrones. Points between $-1 \leq UN \leq +1$ are regarded as stable, those falling between $+1<UN \leq +3$ and $-1>UN \geq -3$ as circadian mobility individuals, while values outside the +3 and −3 range are considered long-range mobility individuals. Sample group 1 (red dots) comprises the samples taken from the earliest forming tissue available for each individual, while sample group 2 (green dots) consists of samples taken from a tissue formed at a later stage than its counterpart from the same individual. (For interpretation of the references to colour in this figure legend, the reader is referred to the Web version of this article.)

data and the surrounding territory's values, while the boundary between local and non-local should be better represented through a more nuanced approach. Moreover, the Unusualness index allows for the assessment of a site's overall population inhomogeneity, as well as the comparison of relative differences between sites.

The application of these methods to the Iron Age case-studies of Fermo and Monterenzio Vecchio, using the ABS isoscape, enabled a re-interpretation of the original binary classification of individuals.

Fermo's results of the Unusualness index revealed clear-cut clusters of individual classification, identifying n = 39 individuals as being stable, n = 11 individuals subject to circadian mobility, and n = 4 to long-range mobility. Some results align with Esposito et al. (2023), identifying a similar number of "non-local" individuals (n = 12 in Esposito et al., 2023), but here these were reclassified as either circadian or long-range mobility individuals in respect to the 10 h isochrone, while the originally "local" individuals were re-classified in either stable or circadian mobility (See Supplementary Material Table S3).

For Monterenzio Vecchio, double sampling (e.g., dm2, M1, P2/M2, M3) allowed a mobility analysis at different life stages. According to the Unusualness index applied to the ABS isoscape isochrones (10 h), n = 13 samples were classified as stable, n = 22 as circadian mobility and n = 9 as long-range mobility. Comparisons with Sorrentino et al. (2018) showed some differences in outcomes, with a reclassification of some originally "non-local" individuals as stable, circadian or long-range mobility individuals. Furthermore, the "local" samples were also differentiated here as either stable or subject to circadian mobility (See Supplementary Material Table S4). Regarding the individuals with double sampling, only n = 3 are classified as stable across both analysed tissues. The majority (n = 6), however, exhibit consistent circadian mobility across samples formed during two distinct life stages, suggesting they spent part of their lives —or at least the periods reflected by the analysed tissues— in locations not entirely coincident with Monterenzio Vecchio and its hinterland. A further n = 4 individuals display a shift from stable to circadian mobility, suggesting an increase in mobility during their lives. Only two individuals present the opposite trend, transitioning from circadian to stable, meaning that their later-life isotopic signatures align more closely with that of Monterenzio Vecchio's hinterland than those representing early life. Another n = 3 individuals exhibit consistent long-range mobility and are therefore interpreted as having spent their childhood and early adolescence in areas isotopically distinct from Monterenzio Vecchio and its surroundings. Finally, n = 1 individual shows a shift from circadian to long range mobility, potentially indicating increased displacement from early childhood to early adolescence.

As previously stated, one of the strengths of the Unusualness index lies in its use as a tool for comparing the population-level inhomogeneity across multiple sites. An example is provided by the comparison between Fermo and Monterenzio Vecchio. To allow for an appropriate comparison, only early-life forming tissues were considered for the latter. The proportion of stable individuals at Fermo (72%) is markedly higher than at Monterenzio (38%), which, in contrast, shows a greater proportion of circadian mobility individuals (43% compared to Fermo's 20%). Although long-range mobility is overall less frequent, it remains higher at Monterenzio Vecchio (19%) than at Fermo (8%), further confirming Monterenzio Vecchio as the site with greater mobility.

Moreover, Table S6 shows that Monterenzio exhibits a higher mean absolute Unusualness value compared to Fermo. To compare the classifications proposed in this study with those presented in the original publications, a mismatch percentage has been calculated (Supplementary Material Table S6). As specified in section 2.3.2, this study's ternary classification was converted into a binary one using two alternative methods: 1. Treating the circadian category as local; 2. Treating the circadian category as non-local. Additionally, individuals originally defined as possible or probable locals/non-locals were treated as certain. Using the first method, classification discrepancies were considerably lower, with a maximum mismatch of 23% in the case of Monterenzio. In contrast, the second binarisation method accentuated the differences, with mismatches reaching up to 45% for Monterenzio.

Overall, Fermo shows a lower percentage of mismatches compared to Monterenzio.

While the approach presented in this study does not fully resolve the equifinality issue —arising from the presence of multiple locations with identical Sr ratios, even beyond the defined walking distances— it provides a way to move beyond a simplistic local/non-local dichotomy. It supports the creation of nuanced mobility categories that can be tailored (adopting different walking time categories, changing the pace parameters, creating new models of mobility) to specific research questions and to the anthropological and archaeological context of the sample under investigation.

Even when adopting a nuanced perspective on mobility, such as the one proposed here, it must still be acknowledged that bulk $^{87}Sr/^{86}Sr$ sampling has been shown to have inherent limitations in accurately determining human (and animal) mobility patterns (Müller and Anczkiewicz, 2016; Willmes et al., 2016; Boethius et al., 2022; Anczkiewicz et al., 2023).

Given the strengths and limitations inherent in isoscapes —the former related to the broader landscape interpolation approach, and the latter to sample distribution and inherent uncertainties— we encourage their improvement and use, while emphasising the need for caution. They are best suited as tools for establishing expected local $^{87}Sr/^{86}Sr$ value ranges in provenance studies but should not be relied upon as the sole reference for determining a local baseline. Isoscapes are thus particularly valuable in previously unexplored regions or as a complementary tool for exploring mobility within a wider isotopic landscape. For optimal reliability in provenance studies, isoscapes should always be complemented by thorough sample distribution analyses and robust baseline datasets (Müller et al., 2024; Esposito et al., 2023; Gigante et al., 2025). Additionally, attention must be paid to prediction variance to assess an isoscape's accuracy and applicability in specific areas. A clear understanding of the sample selection process used in constructing these datasets and related maps is also essential to ensure their proper and effective use. Addressing the potential inaccuracies of isoscapes will require an improved sampling strategy across Italy, targeting under-sampled areas to fill existing gaps. Exploring alternative methodologies, such as Machine Learning, for generating isoscapes could further enhance their precision. At this stage, it is essential to continue testing a combination of methods such as the one employed here, by applying them to additional sites, regions and phases. Expanding such analyses will allow for a more comprehensive evaluation of their effectiveness and a deeper understanding of the suitability of isoscapes for mobility studies.

5. Conclusion

This study highlights the strengths and limitations in the use of isoscapes, isochrones, and the Unusualness index for provenance and mobility studies. Isoscapes are valuable for establishing local $^{87}Sr/^{86}Sr$ ranges, especially in regions with sparse baseline data, but their reliability depends on robust sampling strategies and careful consideration of sample category inclusion. Isochrones and the Unusualness index provide a nuanced framework for assessing mobility, allowing for a more gradual and spatially inclusive approach compared to traditional crow-flight buffer-zone exclusion methods. However, the accuracy of these tools is constrained by the inherent variability in isotopic data and gaps in sampling coverage.

The case-studies from Fermo and Monterenzio Vecchio illustrate how the isochrone and Unusualness index approach to mobility can enhance our understanding of the variability of human movement. These results emphasise the need for continued refinement of sampling strategies, methodological innovations, and further testing across diverse landscapes. By addressing these challenges, isoscapes and related tools can become more reliable for investigating human and animal mobility, ultimately contributing to a deeper understanding of past behaviors and interactions with the environment.

Declaration of generative AI and AI-assisted technologies in the writing process

During the preparation of this work the authors did not use any Generative AI or AI-assisted tool in the writing process and they take full responsibility for the content of the publication.

CRediT authorship contribution statement

Emma Stuart: Conceptualization, Data curation, Formal analysis, Investigation, Methodology, Software, Visualization, Writing – original draft, Writing – review & editing. **Andrea Di Renzoni:** Conceptualization, Data curation, Formal analysis, Methodology, Software, Visualization, Writing – original draft, Writing – review & editing. **Carmen Esposito:** Conceptualization, Writing – original draft, Writing – review & editing. **Luca Bondioli:** Conceptualization, Data curation, Formal analysis, Software, Supervision, Validation, Visualization, Writing – original draft, Writing – review & editing. **Anna Cipriani:** Supervision, Validation, Writing – review & editing. **Alessia Nava:** Funding acquisition, Supervision, Validation, Writing – review & editing. **Federico Lugli:** Data curation, Formal analysis, Investigation, Methodology, Software, Validation, Visualization, Writing – review & editing. **Alessandro Vanzetti:** Conceptualization, Project administration, Supervision, Validation, Writing – review & editing.

Declaration of competing interest

The authors declare that they have no known competing financial interests or personal relationships that could have appeared to influence the work reported in this paper.

Acknowledgements

Carmen Esposito is supported by the European Union's Horizon Europe Research and Innovation programme under the Marie Skłodowska-Curie Actions PF (GA no.101065320 — TULAR). Alessia Nava received funding from the European Research Council (ERC) under the European Union's Horizon Europe Research and Innovation Programme (GA no. 101077348 — MOTHERS; https://erc-mothers.eu/).

Appendix A. Supplementary data

Supplementary data to this article can be found online at https://doi.org/10.1016/j.jas.2026.106561.

Data availability

All the data used in the paper have been uploaded as dataset (.xlsx file) in Zenodo (DOI: https://doi.org/10.5281/zenodo.18566602) with the title: <stuartetal_walking_zenodo>; the elaborations include.docx, .R, QGIS, .xlsx, .png and.jpeg files and are described in the appropriate file named < README_stuartetal_walking>.

References

Adams, S., Grün, R., McGahan, D., Zhao, J., Feng, Y., Nguyen, A., Willmes, M., Quaresimin, M., Lobsey, B., Collard, M., Westaway, M.C., 2019. A strontium isoscape of north-east Australia for human provenance and repatriation. Geoarchaeology 34, 231–251. https://doi.org/10.1002/gea.21728.

Anczkiewicz, R., Nava, A., Bondioli, L., Müller, W., Spötl, C., Koziarska, M., Boczkowska, M., Wojtal, P., Wilczyński, J., 2023. High spatial resolution Sr isotope and trace element record of dental enamel mineralization in a woolly mammoth tooth: implications for paleoecological reconstructions. Quat. Sci. Rev. 313, 108191. https://doi.org/10.1016/j.quascirev.2023.108191.

Arienzo, I., Rucco, I., Di Vito, M.A., D'Antonio, M., Cesarano, M., Carandente, A., De Angelis, F., Romboni, M., Rickards, O., 2020. Sr isotopic composition as a tool for unraveling human mobility in the Campania area. Archaeol. Anthropol. Sci. 12, 157. https://doi.org/10.1007/s12520-020-01088-0.

Bataille, C.P., Crowley, B.E., Wooller, M.J., Bowen, G.J., 2020. Advances in global bioavailable strontium isoscapes. Palaeogeogr. Palaeoclimatol. Palaeoecol. 555, 109849. https://doi.org/10.1016/j.palaeo.2020.109849.

Bataille, C.P., Von Holstein, I.C.C., Laffoon, J.E., Willmes, M., Liu, X.-M., Davies, G.R., 2018. A bioavailable strontium isoscape for Western Europe: a machine learning approach. PLoS One 13, e0197386. https://doi.org/10.1371/journal.pone.0197386.

Bataille, C.P., Bowen, G.J., 2012. Mapping 87Sr/86Sr variations in bedrock and water for large scale provenance studies. Chem. Geol. 304–305, 39–52. https://doi.org/10.1016/j.chemgeo.2012.01.028.

Beard, B.L., Johnson, C.M., 2000. Strontium isotope composition of skeletal material can determine the birth place and geographic mobility of humans and animals. J. Forensic Sci. 45, 1049–1061.

Bentley, R.A., 2006. Strontium isotopes from the Earth to the archaeological skeleton: a review. J. Archaeol. Method Theor 13, 135–187. https://doi.org/10.1007/s10816-006-9009-x.

Boethius, A., Ahlström, T., Kielman-Schmitt, M., Kjällquist, M., Larsson, L., 2022. Assessing laser ablation multi-collector inductively coupled plasma mass spectrometry as a tool to study archaeological and modern human mobility through strontium isotope analyses of tooth enamel. Archaeol. Anthropol. Sci. 14, 97. https://doi.org/10.1007/s12520-022-01556-9.

Bowen, G.J., 2010. Isoscapes: spatial pattern in isotopic biogeochemistry. Annu. Rev. Earth Planet Sci. 38, 161–187. https://doi.org/10.1146/annurev-earth-040809-152429.

Britton, K., Le Corre, M., Willmes, M., Moffat, I., Grün, R., Mannino, M.A., Woodward, S., Jaouen, K., 2020. Sampling plants and malacofauna in 87Sr/86Sr bioavailability studies: implications for isoscape mapping and reconstructing of past mobility patterns. Front. Ecol. Evol. 8, 579473. https://doi.org/10.3389/fevo.2020.579473.

Cabana, G., Clark, J., 2011. Migration in Anthropology: where We Stand, pp. 3–15.

Cameron, C.M., 2013. How people moved among ancient societies: broadening the view. Am. Anthropol. 115, 218–231. https://doi.org/10.1111/aman.12005.

Cangemi, I., 2016. A scale-free, Relational Approach to Social Development in Late-Prehistoric Tyrrhenian Central Italy. PhD thesis Michigan University.

Capo, R.C., Stewart, B., Chadwick, O.A., 1998. Strontium isotopes as tracers of ecosystem processes: theory and methods. Geoderma 82 (1–3), 197–225.

Cavazzuti, C., Cardarelli, A., Quondam, F., Salzani, L., Ferrante, M., Nisi, S., Millard, A. R., Skeates, R., 2019a. Mobile elites at Frattesina: flows of people in a late Bronze Age 'port of trade' in northern Italy. Antiquity 93, 624–644. https://doi.org/10.15184/aqy.2019.59.

Cavazzuti, C., Skeates, R., Millard, A.R., Nowell, G., Peterkin, J., Bernabò Brea, M., Cardarelli, A., Salzani, L., 2019b. Flows of people in villages and large centres in Bronze Age Italy through strontium and oxygen isotopes. PLoS One 14, e0209693. https://doi.org/10.1371/journal.pone.0209693.

Copeland, S.R., Cawthra, H.C., Fisher, E.C., Lee-Thorp, J.A., Cowling, R.M., Le Roux, P.J., Hodgkins, J., Marean, C.W., 2016. Strontium isotope investigation of ungulate movement patterns on the Pleistocene Paleo-Agulhas Plain of the greater cape Floristic Region, South Africa. Quat. Sci. Rev. 141, 65–84. https://doi.org/10.1016/j.quascirev.2016.04.002.

De Laeter, J.R., Böhlke, J.K., De Bièvre, P., Hidaka, H., Peiser, H.S., Rosman, K.J.R., Taylor, P.D.P., 2003. Atomic weights of the elements. Review 2000 (IUPAC Technical Report). Pure Appl. Chem. 75, 683–800. https://doi.org/10.1351/pac200375060683.

Defant, S., Carabia, A., Fetner, R., Craig-Atkins, E., Fernandes, R., Martino, G.P., Costa, S., Sołtysiak, A., Izdebski, A., 2025. Isotopic data reveal a localist Roman population in late Roman Albintimilium, Liguria. Sci. Rep. 15, 12097. https://doi.org/10.1038/s41598-025-92851-7.

DeGroot, M.H., Schervish, M.J., 2012. Probability and Statistics, fourth ed. Addison-Wesley, Boston.

Desideri, J., 2018. Etude de la mobilité des inhumés: analyse des isotopes stables du strontium, de l'oxygène et du carbone. In: De Gattis, G., Curdy, P., Ferroni, A.M., Martinet, F., Poggiani Keller, R., Raiteri, L., Sarti, L., Zidda, G., Mezzena, F. (Eds.), Area Megalitica Di Saint-Martin-de-Corléans. Una Visione Aggiornata. Aosta : Le Château Edizioni, pp. 541–551 (Documenti 13), 2018.

Drennan, R.D., 2009. Statistics for archaeologists. Interdisciplinary Contributions to Archaeology, second ed. Springer, US, Boston, MA. https://doi.org/10.1007/978-1-4419-0413-3.

Dávila, S.G., Martínez Sánchez, R.M., Nederbragt, A., Andersen, M., Madgwick, R., 2024. Tracing the path: first attempt of a multi-isotope approach to animal management in the late Roman city of Torreparedones (Baena, Spain). J. Archaeol. Sci.: Report 60, 104851. https://doi.org/10.1016/j.jasrep.2024.104851.

Emery, M.V., Stark, R.J., Murchie, T.J., Elford, S., Schwarcz, H.P., Prowse, T.L., 2018. Mapping the origins of imperial Roman workers (1st–4th century CE) at Vagnari, Southern Italy, using $^{87}Sr/^{86}Sr$ and $\delta^{18}O$ variability. Am. J. Phys. Anthropol. 166, 837–850. https://doi.org/10.1002/ajpa.23473.

Ericson, J.E., 1985. Strontium isotope characterization in the study of prehistoric human ecology. J. Hum. Evol. 14, 503–514. https://doi.org/10.1016/S0047-2484(85)80029-4.

Esposito, C., Gigante, M., Lugli, F., Miranda, P., Cavazzuti, C., Sperduti, A., Pacciarelli, M., Stoddart, S., Reimer, P., Malone, C., Bondioli, L., Müller, W., 2023. Intense community dynamics in the pre-roman frontier site of Fermo (ninth–fifth century BCE, Marche, central Italy) inferred from isotopic data. Sci. Rep. 13, 3632. https://doi.org/10.1038/s41598-023-29466-3.

Evans, J.A., Montgomery, J., Wildman, G., Boulton, N., 2010. Spatial variations in biosphere $^{87}Sr/^{86}Sr$ in Britain. JGS 167, 1–4. https://doi.org/10.1144/0016-76492009-090.

Francisci, G., Micarelli, I., Iacumin, P., Castorina, F., Di Vincenzo, F., Di Matteo, M., Giostra, C., Manzi, G., Tafuri, M.A., 2020. Strontium and oxygen isotopes as indicators of Longobards mobility in Italy: an investigation at Povegliano Veronese. Sci. Rep. 10, 11678. https://doi.org/10.1038/s41598-020-67480-x.

Frank, A.B., Frei, R., Moutafi, I., Voutsaki, S., Orgeolet, R., Kristiansen, K., Frei, K.M., 2021. The geographic distribution of bioavailable strontium isotopes in Greece – a base for provenance studies in archaeology. Sci. Total Environ. 791, 148156. https://doi.org/10.1016/j.scitotenv.2021.148156.

Frei, K.M., Frei, R., 2011. The geographic distribution of strontium isotopes in Danish surface waters – a base for provenance studies in archaeology, hydrology and agriculture. Appl. Geochem. 26, 326–340. https://doi.org/10.1016/j.apgeochem.2010.12.006.

Frei, R., Frei, K.M., 2013. The geographic distribution of Sr isotopes from surface waters and soil extracts over the island of Bornholm (Denmark) – a base for provenance studies in archaeology and agriculture. Appl. Geochem. 38, 147–160. https://doi.org/10.1016/j.apgeochem.2013.09.007.

Funck, J., Bataille, C., Rasic, J., Wooller, M., 2021. A bio-available strontium isoscape for eastern Beringia: a tool for tracking landscape use of Pleistocene megafauna. J. Quat. Sci. 36, 76–90. https://doi.org/10.1002/jqs.3262.

Gigante, M., Esposito, C., Lugli, F., Sperduti, A., Cinquantaquattro, T.E., d'Agostino, B., Nava, A., Müller, W., Bondioli, L., 2025. Where Typhoeus lived: 87Sr/86Sr analysis of human remains in the first Greek site in the Western Mediterranean, Pithekoussai, Italy. iScience 28, 111927. https://doi.org/10.1016/j.isci.2025.111927.

Gigante, M., Mazzariol, A., Bonetto, J., Armaroli, E., Cipriani, A., Lugli, F., 2023. Machine learning-based Sr isoscape of southern Sardinia: a tool for bio-geographic studies at the Phoenician-Punic site of Nora. PLoS One 18, e0287787. https://doi.org/10.1371/journal.pone.0287787.

Gregoricka, L.A., 2021. Moving forward: a bioarchaeology of mobility and migration. J. Archaeol. Res. 29, 581–635. https://doi.org/10.1007/s10814-020-09155-9.

Grupe, G., Klaut, D., Mauder, M., Kröger, P., Lang, A., Mayr, C., Söllner, F., 2018. Multi-isotope provenancing of archaeological skeletons including cremations in a reference area of the European Alps. Rapid Commun. Mass Spectrom. 32, 1711–1727. https://doi.org/10.1002/rcm.8218.

Hamilton, M., Nelson, S.V., Fernandez, D.P., Hunt, K.D., 2019. Detecting riparian habitat preferences in "savanna" chimpanzees and associated Fauna with strontium isotope ratios: implications for reconstructing habitat use by the chimpanzee-human last common ancestor. Am. J. Phys. Anthropol. 170, 551–564. https://doi.org/10.1002/ajpa.23932.

Hartman, G., Richards, M., 2014. Mapping and defining sources of variability in bioavailable strontium isotope ratios in the Eastern Mediterranean. Geochem. Cosmochim. Acta 126, 250–264. https://doi.org/10.1016/j.gca.2013.11.015.

Hedges, R.E.M., 2002. Bone diagenesis: an overview of processes. Archaeometry 44, 319–328. https://doi.org/10.1111/1475-4754.00064.

Hedman, K.M., Slater, P.A., Fort, M.A., Emerson, T.E., Lambert, J.M., 2018. Expanding the strontium isoscape for the American midcontinent: identifying potential places of origin for Cahokian and pre-columbian migrants. J. Archaeol. Sci.: Report 22, 202–213. https://doi.org/10.1016/j.jasrep.2018.09.027.

Herzog, I., 2020. Spatial analysis based on cost functions. In: Gillings, M., Hacıgüzeller, P., Lock, G. (Eds.), Archaeological Spatial Analysis. Routledge, pp. 333–358. https://doi.org/10.4324/9781351243858-18.

Holt, E., Evans, J.A., Madgwick, R., 2021. Strontium (87Sr/86Sr) mapping: a critical review of methods and approaches. Earth Sci. Rev. 216, 103593. https://doi.org/10.1016/j.earscirev.2021.103593.

Holt, E., Lugli, F., Schirru, D., Gigante, M., Faillace, K., Millet, M.-A., Andersen, M., Madgwick, R., 2025. Comparing machine learning isoscapes of 87Sr/86Sr ratios of plants on the island of Sardinia: implications for the use of isoscapes for assessing the provenance of biological specimens. Sci. Total Environ. 989, 179880. https://doi.org/10.1016/j.scitotenv.2025.179880.

Janzen, A., Bataille, C., Copeland, S.R., Quinn, R.L., Ambrose, S.H., Reed, D., Hamilton, M., Grimes, V., Richards, M.P., Le Roux, P., Roberts, P., 2020. Spatial variation in bioavailable strontium isotope ratios (87Sr/86Sr) in Kenya and northern Tanzania: implications for ecology, paleoanthropology, and archaeology. Palaeogeogr. Palaeoclimatol. Palaeoecol. 560, 109957. https://doi.org/10.1016/j.palaeo.2020.109957.

Killgrove, K., Montgomery, J., 2016. All roads lead to Rome: exploring human migration to the eternal City through biochemistry of skeletons from two imperial-era cemeteries (1st-3rd c AD). PLoS One 11, e0147585. https://doi.org/10.1371/journal.pone.0147585.

Knipper, C., 2009. Mobility in a sedentary society: insights from isotope analysis of LBK human and animal teeth. In: Creating Communities: New Advances in Central European Neolithic Research, pp. 142–158.

Knudson, K.J., Williams, H.M., Buikstra, J.E., Tomczak, P.D., Gordon, G.W., Anbar, A.D., 2010. Introducing δ88/86Sr analysis in archaeology: a demonstration of the utility of strontium isotope fractionation in paleodietary studies. J. Archaeol. Sci. 37, 2352–2364. https://doi.org/10.1016/j.jas.2010.04.009.

Kootker, L.M., Van Lanen, R.J., Kars, H., Davies, G.R., 2016. Strontium isoscapes in the Netherlands. Spatial variations in 87Sr/86Sr as a proxy for palaeomobility. J. Archaeol. Sci.: Report 6, 1–13. https://doi.org/10.1016/j.jasrep.2016.01.015.

Ladegaard-Pedersen, P., Frei, R., Frank, A.B., Saracino, M., Zorzin, R., Martinelli, N., Kaul, F., Kristiansen, K., Frei, K.M., 2022. Constraining a bioavailable strontium isotope baseline for the Lake Garda region, Northern Italy: a multi-proxy approach. J. Archaeol. Sci.: Report 41, 103339. https://doi.org/10.1016/j.jasrep.2022.103339.

Laffoon, J.E., Sonnemann, T.F., Shafie, T., Hofman, C.L., Brandes, U., Davies, G.R., 2017. Investigating human geographic origins using dual-isotope (87Sr/86Sr, δ18O) assignment approaches. PLoS One 12, e0172562. https://doi.org/10.1371/journal.pone.0172562.

Langmuir, E., 1984. Mountaincraft and leadership. The Scottish Sports Council/MLTB, Cordee, Leicester.
Lazzerini, N., Balter, V., Coulon, A., Tacail, T., Marchina, C., Lemoine, M., Bayarkhuu, N., Turbat, Ts, Lepetz, S., Zazzo, A., 2021. Monthly mobility inferred from isoscapes and laser ablation strontium isotope ratios in caprine tooth enamel. Sci. Rep. 11, 2277. https://doi.org/10.1038/s41598-021-81923-z.
Lee-Thorp, J., Sealy, J., 2008. Beyond documenting diagenesis: the fifth international bone diagenesis workshop. Palaeogeogr. Palaeoclimatol. Palaeoecol. 266, 129–133. https://doi.org/10.1016/j.palaeo.2008.03.025.
Lollini, D., 1976. La civiltà picena. In: Cianfarani, V., et al. (Eds.), Popoli E Civiltà Dell'Italia Antica. Biblioteca di Storia Patria, pp. 107–195.
Lugli, F., Cipriani, A., Bruno, L., Ronchetti, F., Cavazzuti, C., Benazzi, S., 2022. A strontium isoscape of Italy for provenance studies. Chem. Geol. 587, 120624. https://doi.org/10.1016/j.chemgeo.2021.120624.
Madgwick, R., Lamb, A.L., Sloane, H., Nederbragt, A.J., Albarella, U., Pearson, M.P., Evans, J.A., 2019. Multi-isotope analysis reveals that feasts in the Stonehenge environs and across Wessex drew people and animals from throughout Britain. Sci. Adv. 5. https://doi.org/10.1126/sciadv.aau6078 eaau6078.
Maurer, A.-F., Galer, S.J.G., Knipper, C., Beierlein, L., Nunn, E.V., Peters, D., Tütken, T., Alt, K.W., Schöne, B.R., 2012. Bioavailable 87Sr/86Sr in different environmental samples — effects of anthropogenic contamination and implications for isoscapes in past migration studies. Sci. Total Environ. 433, 216–229. https://doi.org/10.1016/j.scitotenv.2012.06.046.
Müller, W., Lugli, F., McCormack, J., Evans, D., Anczkiewicz, R., Bondioli, L., Nava, A., 2024. Human life histories. In: Treatise on Geochemistry, third ed. Elsevier, pp. 281–328.
Müller, W., Anczkiewicz, R., 2016. Accuracy of laser-ablation (LA)-MC-ICPMS Sr isotope analysis of (bio)apatite – a problem reassessed. J. Anal. At. Spectrom. 31, 259–269. https://doi.org/10.1039/C5JA00311C.
Montgomery, J., Evans, J.A., Wildman, G., 2006. 87Sr/86Sr isotope composition of bottled British mineral waters for environmental and forensic purposes. Appl. Geochem. 21, 1626–1634. https://doi.org/10.1016/j.apgeochem.2006.07.002.
Motta, L., Beydler, K., 2021. 19. Agriculture in Iron Age and archaic Italy. In: Hollander, D., Howe, T. (Eds.), A Companion to Ancient Agriculture, vol 2021. John Wiley & Sons, , New York, pp. 399–415.
Nava, A., Lugli, F., Romandini, M., Badino, F., Evans, D., Helbling, A.H., Oxilia, G., Arrighi, S., Bortolini, E., Delpiano, D., Duches, R., Figus, C., Livraghi, A., Marciani, G., Silvestrini, S., Cipriani, A., Giovanardi, T., Pini, R., Tuniz, C., Bernardini, F., Dori, I., Coppa, A., Cristiani, E., Dean, C., Bondioli, L., Peresani, M., Müller, W., Benazzi, S., 2020. Early life of neanderthals. Proc. Natl. Acad. Sci. U. S. A. 117, 28719–28726. https://doi.org/10.1073/pnas.2011765117.
Nelson, B.K., Deniro, M.J., Schoeninger, M.J., De Paolo, D.J., Hare, P.E., 1986. Effects of diagenesis on strontium, carbon, nitrogen and oxygen concentration and isotopic composition of bone. Geochem. Cosmochim. Acta 50, 1941–1949. https://doi.org/10.1016/0016-7037(86)90250-4.
Ortalli, J., 1990. Nuovi dati sul popolamento di età celtica nel territorio bolognese. Études Celt. 27, 7–41, 1990.
Pallottino, M., 1984. Etruscologia, seventh ed. Hoepli, Milano.
Parker, R.B., 1968. Electron microprobe analysis of fossil bones and teeth. Geol. Soc. Am. Spec. Pap. 101, 415–416.
Parker, R.B., Toots, H., 1970. Minor elements in fossil bone. Geol. Soc. Am. Bull. 81, 925. https://doi.org/10.1130/0016-7606(1970)81[925:MEIFB]2.0.CO;2.
Pestle, W.J., Simonetti, A., Curet, L.A., 2013. 87Sr/86Sr variability in Puerto Rico: geological complexity and the study of paleomobility. J. Archaeol. Sci. 40, 2561–2569. https://doi.org/10.1016/j.jas.2013.01.020.
R Core Team, 2025. R: A language and environment for statistical computing. R Foundation for Statistical Computing. http://www.r-project.org.
Reinberger, K.L., Reitsema, L.J., Kyle, B., Vassallo, S., Kamenov, G., Krigbaum, J., 2021. Isotopic evidence for geographic heterogeneity in Ancient Greek military forces. PLoS One 16, e0248803. https://doi.org/10.1371/journal.pone.0248803.
Richards, M.P., Mannino, M.A., Jaouen, K., Dozio, A., Hublin, J.-J., Peresani, M., 2021. Strontium isotope evidence for Neanderthal and modern human mobility at the upper and middle palaeolithic site of Fumane Cave (Italy). PLoS One 16, e0254848. https://doi.org/10.1371/journal.pone.0254848.
Romboni, M., Arienzo, I., Di Vito, M.A., Lubritto, C., Piochi, M., Di Cicco, M.R., Rickards, O., Rolfo, M.F., Sevink, J., De Angelis, F., Alessandri, L., 2023. La Sassa cave: isotopic evidence for Copper Age and Bronze Age population dynamics in Central Italy. PLoS One 18, e0288637. https://doi.org/10.1371/journal.pone.0288637.
Rossi, M., Iacumin, P., Venturelli, G., 2024. 87Sr/86Sr isotope ratio as a tool in archaeological investigation: limits and risks. Quaternary 7, 6. https://doi.org/10.3390/quat7010006.
Sabatini, S., Frei, K.M., De Grossi Mazzorin, J., Cardarelli, A., Pellacani, G., Frei, R., 2022. Investigating sheep mobility at Montale, Italy, through strontium isotope analyses. J. Archaeol. Sci.: Report 41, 103298. https://doi.org/10.1016/j.jasrep.2021.103298.
Scaffidi, B.K., Knudson, K.J., 2020. An archaeological strontium isoscape for the prehistoric Andes: understanding population mobility through a geostatistical meta-analysis of archaeological 87Sr/86Sr values from humans, animals, and artifacts. J. Archaeol. Sci. 117, 105121. https://doi.org/10.1016/j.jas.2020.105121.
Scheeres, M., Knipper, C., Hauschild, M., Schönfelder, M., Siebel, W., Vitali, D., Pare, C., Alt, K.W., 2013. Evidence for "Celtic migrations"? Strontium isotope analysis at the early La Tène (LT B) cemeteries of Nebringen (Germany) and Monte Bibele (Italy). J. Archaeol. Sci. 40, 3614–3625. https://doi.org/10.1016/j.jas.2013.05.003.
Schoeninger, M.J., 1979a. Dietary reconstruction at chalcatzingo: a formative period site in Morelos, Mexico. U OF M Museum Anthro Archaeology. https://doi.org/10.3998/mpub.11394767. Ann Arbor, MI.
Schoeninger, M.J., 1979b. Diet and status at Chalcatzingo: some empirical and technical aspects of strontium analysis. Am. J. Phys. Anthropol. 51, 295–309. https://doi.org/10.1002/ajpa.1330510302.
Schwartz, C.W., Somerville, A.D., Nelson, B.A., Knudson, K.J., 2021. Investigating Pre-Hispanic scarlet macaw origins through radiogenic strontium isotope analysis at Paquimé in Chihuahua, Mexico. J. Anthropol. Archaeol. 61, 101256. https://doi.org/10.1016/j.jaa.2020.101256.
Sillen, A., 1981. Strontium and diet at hayonim Cave. Am. J. Phys. Anthropol. 56, 131–137. https://doi.org/10.1002/ajpa.1330560204.
Sillen, A., Sealy, J.C., 1995. Diagenesis of Strontium in Fossil Bone: a Reconsideration of Nelson et al.(1986). J. Archaeol. Sci. 22, 313–320. https://doi.org/10.1006/jasc.1995.0033.
Slovak, N.M., Paytan, A., 2011. Applications of Sr isotopes in archaeology. Adv. Isotope Geochem. Springer Berlin Heidelberg, Berlin, Heidelberg, ISBN 9783642106361, pp. 743–768. https://doi.org/10.1007/978-3-642-10637-8_35. http://link.springer.com/10.1007/978-3-642-10637-8_35. (Accessed 30 June 2011).
Snoeck, C., Ryan, S., Pouncett, J., Pellegrini, M., Claeys, P., Wainwright, A.N., Mattielli, N., Lee-Thorp, J.A., Schulting, R.J., 2020. Towards a biologically available strontium isotope baseline for Ireland. Sci. Total Environ. 712, 136248. https://doi.org/10.1016/j.scitotenv.2019.136248.
Sorrentino, R., Bortolini, E., Lugli, F., Mancuso, G., Buti, L., Oxilia, G., Vazzana, A., Figus, C., Serrangeli, M.C., Margherita, C., Penzo, A., Gruppioni, G., Gottarelli, A., Jochum, K.P., Belcastro, M.G., Cipriani, A., Feeney, R.N.M., Benazzi, S., 2018. Unravelling biocultural population structure in 4th/3rd century BC Monterenzio Vecchio (Bologna, Italy) through a comparative analysis of strontium isotopes, non-metric dental evidence, and funerary practices. PLoS One 13, e0193796. https://doi.org/10.1371/journal.pone.0193796.
Tarquini, S., Isola, I., Favalli, M., Battistini, A., Dotta, G., 2023. TINITALY, a digital elevation model of Italy with a 10 meters cell size, Version 1.1. https://doi.org/10.13127/TINITALY/1.1.
Tchebichef, P., 1867. Des valeurs moyennes. J. Math. Pure Appl. 2 (12), 177–184.
Toots, H., Voorhies, M.R., 1965. Strontium in fossil bones and the reconstruction of food chains. Science 149, 854–855. https://doi.org/10.1126/science.149.3686.854.
Torelli, M., 1986. La storia. In: Pallottino, M., et al. (Eds.), Rasenna – Storia E Civiltà Degli Etruschi. Garzanti/Scheiwiller, pp. 15–76.
Trentacoste, A., Lightfoot, E., Le Roux, P., Buckley, M., Kansa, S.W., Esposito, C., Gleba, M., 2020. Heading for the hills? A multi-isotope study of sheep management in first-millennium BC Italy. J. Archaeol. Sci.: Report 29, 102036. https://doi.org/10.1016/j.jasrep.2019.102036.
Trickett, M.A., Budd, P., Montgomery, J., Evans, J., 2003. An assessment of solubility profiling as a decontamination procedure for the 87Sr/86Sr analysis of archaeological human skeletal tissue. Appl. Geochem. 18, 653–658. https://doi.org/10.1016/S0883-2927(02)00181-6.
Vita-Finzi, C., Higgs, E.S., Sturdy, D., Harriss, J., Legge, A.J., et al., 1970. Prehistoric economy in the Mount Carmel Area of Palestine: site catchment analysis. Proc. Prehist. Soc. 36, 1–37. https://doi.org/10.1017/s0079497x00013074. https://www.cambridge.org/core/product/identifier/S0079497X00013074/type/journal_article. (Accessed 6 September 2016).
Wang, X., Bocksberger, G., Lautenschläger, T., Finckh, M., Meller, P., O'Malley, G.E., Oelze, V.M., 2023. A bioavailable strontium isoscape of Angola with implications for the archaeology of the transatlantic slave trade. J. Archaeol. Sci. 154, 105775. https://doi.org/10.1016/j.jas.2023.105775.
Wang, X., Tang, Z., 2020. The first large-scale bioavailable Sr isotope map of China and its implication for provenance studies. Earth Sci. Rev. 210, 103353. https://doi.org/10.1016/j.earscirev.2020.103353.
Washburn, E., Nesbitt, J., Ibarra, B., Fehren-Schmitz, L., Oelze, V.M., 2021. A strontium isoscape for the Conchucos region of highland Peru and its application to Andean archaeology. PLoS One 16, e0248209. https://doi.org/10.1371/journal.pone.0248209.
Willmes, M., 2015. Strontium Isotope Tracing of Prehistoric Human Mobility in France (Phd Thesis).
Willmes, M., Bataille, C., James, H., Moffat, I., McMorrow, L., Kinsley, L., Armstrong, R., Eggins, S., Grün, R., 2021. Mapping of bioavailable strontium isotope ratios in France for archaeological provenance studies. https://doi.org/10.31219/osf.io/txasq.
Willmes, M., Kinsley, L., Moncel, M.-H., Armstrong, R.A., Aubert, M., Eggins, S., Grün, R., 2016. Improvement of laser ablation in situ micro-analysis to identify diagenetic alteration and measure strontium isotope ratios in fossil human teeth. J. Archaeol. Sci. 70, 102–116. https://doi.org/10.1016/j.jas.2016.04.017.
Wright, L.E., 2005. Identifying immigrants to Tikal, Guatemala: defining local variability in strontium isotope ratios of human tooth enamel. J. Archaeol. Sci. 32, 555–566. https://doi.org/10.1016/j.jas.2004.11.011.
Yanes, Y., Delgado, A., Castillo, C., Alonso, M.R., Ibáñez, M., De La Nuez, J., Kowalewski, M., 2008. Stable isotope (δ18O, δ13C, and δD) signatures of recent terrestrial communities from a low-latitude, oceanic setting: endemic land snails, plants, rain, and carbonate sediments from the eastern Canary Islands. Chem. Geol. 249, 377–392. https://doi.org/10.1016/j.chemgeo.2008.01.008.
Zaugg, C., Guggisberg, M.A., Vach, W., Cooper, M.J., Gerling, C., 2023. Mapping strontium isotope geographical variability as a basis for multi-regional human mobility: the Sybaris Region (S Italy) in the early 1st millennium BC. Environ. Archaeol. 1–19. https://doi.org/10.1080/14614103.2023.2260622.